表1　構造遺伝子の種によって分類されるサブステム

u	ヒト
o	マウス
a	ラット
e	ハムスター
i	霊長類
xi	キメラ
zu	ヒト化
axo	ラット・マウスハイブリッド

表2　対象疾患および標的部位によって分類されるサブステム

-ba(c)-	バクテリア
-os-*1	骨
-ci(r)-	心臓血管
-le(s)-	炎症性病変
-li(m)-	免疫調節
-vi(r)-	ウイルス

*1 暫定サブステム

表3　腫瘍の種類によって分類されるサブステム

-co(l)-	大腸がん
-go(t)-	精巣がん
-go(v)-	卵巣がん
-ma(r)-	乳がん
-me(l)-	黒色腫
-pr(o)-	前立腺がん
-tu(m)-	その他腫瘍全体

後その数は増大すると予想されている。

モノクローナル抗体のステム「**-mab**」は，構造遺伝子の由来(種)によってサブステムに分類される(**表1**)。さらに，対象疾患や標的部位，または対象とする腫瘍の種類によってもサブステムがつけられる(**表2**，**表3**)。

放射性ラベル化合物や合成化合物が共有結合したモノクローナル抗体には，抗体名の後にその化合物の名前をつける。モノクローナル抗体を放射性同位体のキャリアとして用いる場合は，放射性同位体のINNを抗体名の前につける(例，Technetium(^{99m}Tc)Pintumomab)。また，毒素(toxin)を共有結合したモノクローナル抗体には，「**-toxa-**」をつける。

(1)「-omab」：マウスモノクローナル抗体

「**-omab**」は，マウスモノクローナル抗体(mouse monoclonal antibody)を示す。JANには**Iburitumomab** Tiuxetan(イブリ**ツモマブ** チウキセタン)が収載されている(**図3**)。イブリ**ツモマブ**はB細胞性の悪性リンパ腫に多く発現しているCD20を認識するIgG1で，腫瘍を標的とすることを示すサブステム「**-tu(m)-**」を持つ。金属キレート剤であるチウキセタンが共有結合したイブリ**ツモマブ** チウキセタンは，放射性同位元素と組み合わせることによって，CD20を認識し，B細胞を死滅させる。イブリ**ツモマブ** チウキセタンはCD20陽性のB細胞性非ホジキンリンパ腫治療薬として2002年に米国で承認されている。日本では希少疾病用医薬品等指定品目の1つとなっている。

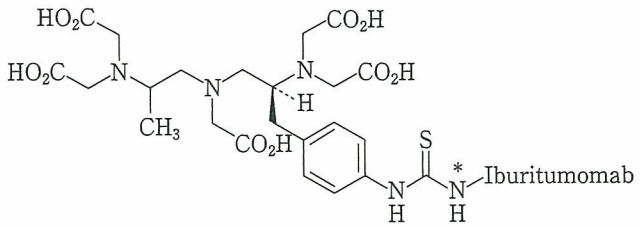

図3　Iburitumomab Tiuxetan(イブリツモマブ チウキセタン)の構造(日本承認申請中)

他に「**-omab**」をサブステムに持つ品目として41種類の抗体がINNに収載されている。

(2)「-ximab」：キメラモノクローナル抗体

「**-ximab**」は，キメラモノクローナル抗体(chimeric monoclonal antibody)を示す。現在，日本で承認されている医薬品には，以下の3品目がある。

Basi**liximab**(Genetical Recombination)(バシ**リキシマブ**(遺伝子組換え))

Infli**ximab**(Genetical Recombination)(インフ**リキシマブ**(遺伝子組換え))

Ri**tuximab**(Genetical Recombination)(リ**ツキシマブ**(遺伝子組換え))

バシ**リキシマブ**は活性化T細胞表面のインターロイキン(IL)-2受容体α鎖(CD25)を標的とするIgG1で，IL-2によって誘導されるリンパ球の分化・増殖を抑制する。腎移植後の急性拒絶反応抑制薬として2002年に承認された。免疫機能調節薬を示すサブステム「**-li-**」を持つ。

インフ**リキシマブ**は腫瘍壊死因子(TNF-α，Tumor necrosis factor-α，本稿で紹介するステム48(1)「TNF-α阻害薬」を参照)を標的とするIgG1で，クローン病治療薬として利用されている(2002年承認)。また，現在，ベーチェット病による難治性網膜ぶどう膜炎治療薬として希少疾病用医薬品の指定を受けている。免疫機能調節薬を示すサブステム「**-li-**」を持つ。

リ**ツキシマブ**はCD20を標的分子とするIgG1で，2001年にCD20陽性のB細胞性非ホジキンリンパ腫の治療薬として承認された。腫瘍を標的とすることを示すサブステム「**-tu-**」がつけられている。

これ以外にJANに収載されている医薬品として以下の品目がある。

Ab**ciximab**(Genetical Recombination)(アブ**シキシマブ**(遺伝子組換え))

Ce**tuximab**(Genetical Recombination)(セ**ツキシマブ**

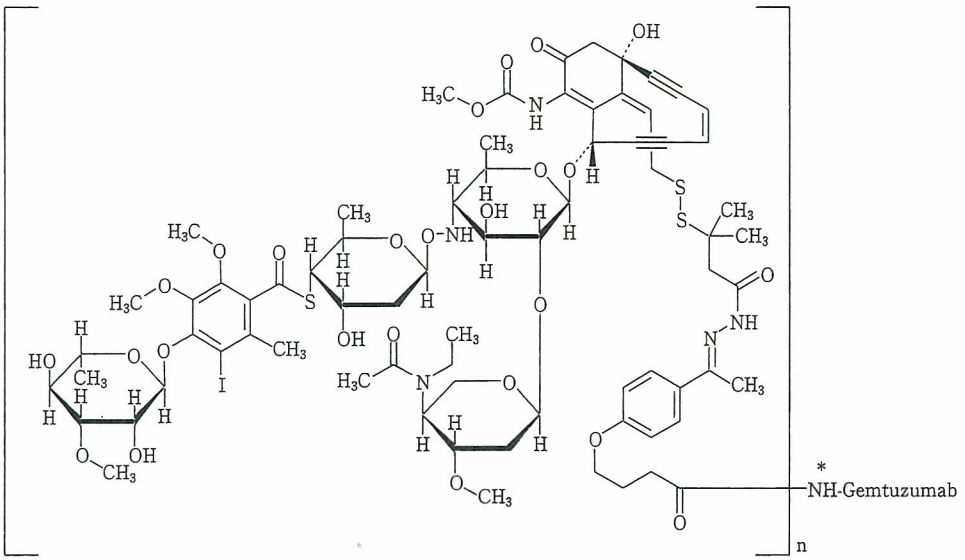

図4　Gemtuzumab Ozogamicin(ゲムツズマブ オゾガマイシン)の構造(2005年日本承認)

(遺伝子組換え))

アブ**シキシマブ**は血小板膜に発現するインテグリン$\alpha 2\beta 3$を認識するIgG1で，Fab部分のみからなる。米国では1994年に経皮的冠動脈形成術後の再狭窄治療薬として承認されている。サブステム「**-ci-**」は心臓血管を標的とすることを意味する。

セ**ツキシマブ**はEGF受容体を認識するIgG1で，米国では大腸がん治療薬として2004年に承認された。腫瘍を標的とするサブステム「**-tu-**」を持つ。

2006年6月現在，INNにはこれらの品目を含む15品目が収載されている。

(3)「-zumab」：ヒト化モノクローナル抗体

「**-zumab**」は，ヒト化モノクローナル抗体(humanized monoclonal antibody)を示す。現在，日本で承認されている医薬品には，以下の4品目がある。

Gem**tuzumab** Ozogamicin(Genetical Recombination)(ゲム**ツズマブ** オゾガマイシン(遺伝子組換え))

Pali**vizumab**(Genetical Recombination)(パリ**ビズマブ**(遺伝子組換え))

Toci**lizumab**(Genetical Recombination)(トシ**リズマブ**(遺伝子組換え))

Tras**tuzumab**(Genetical Recombination)(トラス**ツズマブ**(遺伝子組換え))

ゲム**ツズマブ**は急性骨髄性白血病細胞の細胞表面抗原CD33を認識するIgG4で，腫瘍を標的とする抗体を示すサブステム「**-tu-**」を持つ。**図4**にゲム**ツズマブ**のリジン残基にオゾガマイシンがアミド結合したゲム**ツズマブ**オゾガマイシンの構造を示す。この医薬品は，白血病細胞のCD33に結合して細胞内に取り込まれると，リソソーム内で分解されてオゾガマイシンを遊離し，細胞を傷害する。ゲム**ツズマブ** オゾガマイシンは再発または難治性のCD33陽性の急性骨髄性白血病治療薬として2005年に承認された。

パリ**ビズマブ**はRSウイルス(respiratory syncytial virus)Fタンパク質を認識するIgG1で，小児RSウイルス感染治療薬として2002年に承認された。サブステム「**-vi-**」はウイルスを標的としていることを示す。

トシ**リズマブ**はIL-6受容体を認識するIgG1で，2005年，わが国において世界に先駆けてキャッスルマン病治療薬として承認された。キャッスルマン病は腫瘍リンパ節から大量のIL-6が産生されるリンパ増殖性疾患で，症状および病態にIL-6が関わっている。トシ**リズマブ**はIL-6とその受容体の結合を競合的に阻害する。免疫機能調節作用を示すサブステム「**-li-**」を持つ。関節リウマチ治療薬としての承認申請に向けて，臨床第Ⅲ相試験が実施されている。

トラス**ツズマブ**は乳がんに過剰発現するHER2を認識するIgG1で，HER2陽性転移性乳がん治療薬として2001年に承認された。HER2に結合してシグナルが細胞内に伝わるのを阻害するとともに，免疫細胞を呼び寄せがん細胞を破壊する。腫瘍を標的とすることを示すサブステム「**-tu-**」を持つ。

「**-zumab**」を持つ他の品目としてJANには以下の2品目が収載されている。

Oma**lizumab**(Genetical Recombination)(オマ**リズマ**

ブ(遺伝子組換え))

Bevacizumab(Genetical Recombination)(ベバシズマブ(遺伝子組換え))

オマリズマブはヒトIgEモノクローナル抗体を認識するIgG1で，米国では2003年にぜんそく治療薬として承認されている。免疫機能調節作用を示すサブステム「-li-」を持つ。本邦では承認申請中である。

ベバシズマブはVEGFを認識するIgG1で，米国では大腸がん治療薬として2004年に承認されている。作用部位が心臓血管系であることを示すサブステム「-ci-」を持つ。日本では承認申請中である。

2006年6月現在，INNにはこれらの品目を含む47品目が収載されている。この数は今後さらに増大することが予想される。

(4)「-umab」：ヒトモノクローナル抗体

「-umab」は，ヒトモノクローナル抗体(human monoclonal antibody)を示す。JANには以下の2品目が収載されている。

Adalimumab(Genetical Recombination)(アダリムマブ(遺伝子組換え))

Regavirumab(レガビルマブ)

アダリムマブはTNF-αを認識するIgG1で，免疫機能調節作用を示す「-li(m)-」を持つ。クローン病および慢性リウマチ治療薬として2003年に米国で承認されている。わが国ではインフリキシマブおよびエタネルセプト(後述)に続く第3のTNF-α阻害薬として承認申請中である。

レガビルマブはヒトヘルペスウイルスを認識するIgG1で，ウイルスに作用することを示す「-vi(r)-」を持つ。免疫低下時におけるサイトメガロウイルス感染症，悪性腫瘍，後天性免疫不全症候群等を対象とした希少疾病用医薬品等指定品目であったが，現在では取り消されている。

他に「-umab」をサブステムに持つ品目として29種類の抗体がINNに収載されている。

ステム48 「-cept」：受容体分子

「-cept」は，受容体分子(receptor molecule)に共通のステムである。受容体のターゲット分子を示す文字を「-cept」の前に挿入する。

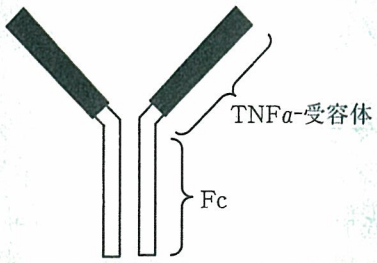

図5　Etanercept(エタネルセプト)の構造(2005年日本承認)

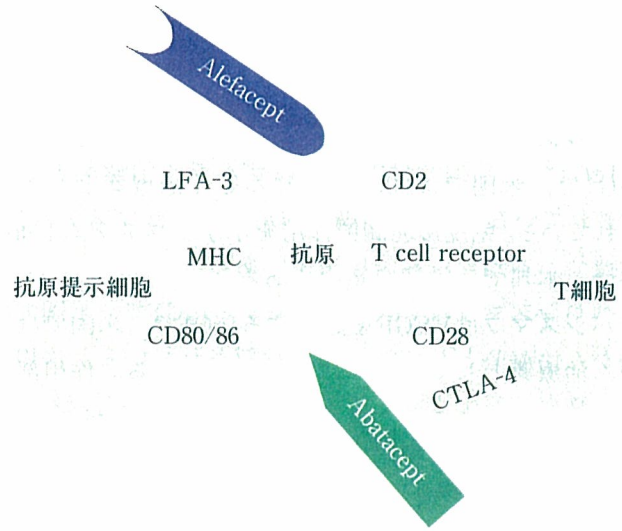

図6　抗原提示細胞およびT細胞の結合，ならびにAlefaceptおよびAbataceptの作用機構

(1)「-nercept」：TNF-α阻害薬

「-nercept」は，TNF-α阻害薬(Tumor necrosis factor antagonist)に共通のステムである。

TNF-αは，活性化マクロファージなどが産生するサイトカインの一種で，当初は腫瘍部位に出血性の壊死を誘導する因子として発見されたが，現在では，炎症を通した生体防御制御に関わる因子と考えられている。体内にはTNF-αの受容体として，細胞表面のTNF-α受容体(単量体)と可溶性TNF-α受容体(単量体)が存在する。細胞表面の受容体にTNF-αが結合すると炎症反応が惹起される。関節リウマチ患者の関節内では，TNF-αが異常に増加し，可溶性TNF-α受容体が不足しているため，炎症反応が増大されて関節軟骨や骨の破壊が進行するといわれている。

TNF-α阻害薬は可溶性TNF-α受容体よりも強い力でTNF-αと結合し，TNF-αが細胞表面のTNF-α受容体に結合するのを阻止する作用を持つ。TNF-α阻害薬として日本で承認されているものにEtanercept(エタネルセプト)がある。なお，TNF-α阻害薬として他にインフリキシマブがあるが，インフリキシマブには前述したように，キメラモノクローナル抗体のステム「-ximab」が与えられている(ステム47(2)参照)。

エタネルセプトは，TNF-α受容体とIgG1のFc領域から構成されるサブユニットがホモダイマーを形成した遺伝子組換え型融合糖タンパク質である(図5)。可溶性受容体より強くTNF-αと結合し，炎症を抑制する。日本ではリウマチ疾患治療薬として2005年に承認された。

「-nercept」をステムに持ち，INNに収載されているその他の品目にLenercept，Onercept，およびPegsunerceptがある。

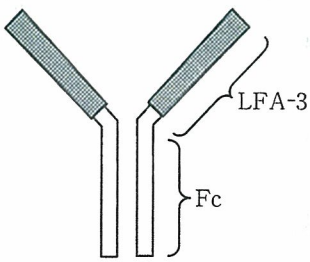

図7　Alefaceptの構造(日本未承認)

(2)「-lefacept」：リンパ球機能関連抗原3(LFA-3)

「-lefacept」はリンパ球機能関連抗原3(leukocyte function antigen-3，LFA-3)を示すステムである。

体内へ侵入した外来異物は，断片化され，抗原提示細胞表面の主要組織適合抗原(MHC)に捕捉されて細胞表面に提示される。T細胞は，このMHC複合体を異物と認識して活性化する。乾癬は，異物がないのにT細胞が活性化し，IL-1やTNF-αなどのサイトカインが放出され，皮膚などに炎症反応が惹起されている疾患である。LFA-3は抗原提示細胞表面に発現し，T細胞表面のCD2と結合するタンパク質で，抗原提示細胞とT細胞の結合に不可欠な分子の1つである(図6)。

INNにはステム「-lefacept」を持つ医薬品としてAlefaceptが収載されている。Alefaceptは，図7に示すように，LFA-3のCD2結合部位とIgG1のFc部分を融合した2量体タンパク質で，T細胞表面のCD2に結合し，T細胞が抗原提示細胞に結合して活性化することを抑制

する(図6)。また，IgG部分を利用してナチュラルキラー細胞やマクロファージを呼び寄せT細胞を破壊する。2003年，**Alefacept**は米国で中程度から重症の成人尋常性乾癬治療薬として承認された。

(3)「-cocept」：補体受容体

補体受容体(complement receptor)には「**-co-**」をつける。INNには**Mirococept**が収載されている。**Mirococept**は脂溶性のペプチドモチーフを結合した可溶性補体受容体1の断片である。臨床試験は休止されている。

(4)「-farcept」：インターフェロン受容体

インターフェロン受容体(interferon receptor)には「**-far-**」をつける。INNには**Bifarcept**が登録されている。**Bifarcept**はI型インターフェロン(インターフェロンα/β)受容体断片である。

(5)「-vircept」：抗ウイルス受容体

抗ウイルス受容体(anti-viral receptor)には「**-vir-**」をつける。INNには**Alvircept** Sudotoxが収載されている。**Alvircept** SudotoxはT細胞上に発現するCD4で，I型ヒト免疫不全ウイルス(HIV-1)のエンベロープ糖タンパクgp120の受容体である。

(6)「-bercept」：血管内皮成長因子受容体

血管内皮成長因子受容体(vascular endothelial growth factor receptor)には「**-ber-**」をつける。現在INN収載品目はない。

(7)その他

その他の受容体分子としてINNには**Abatacept**，**Belatacept**，**Atacicept**が収載されている。

Abataceptは，ヒトT細胞上の調節タンパク質の1つであるCTLA-4(cytotoxic T lymphocyte-associated antigen 4)の細胞外ドメインとIgG1のFc領域を融合したタンパク質である(**図8**)。前述したように，T細胞の活性化には，T細胞が抗原提示細胞上の抗原ペプチドを認識し，T細胞にシグナルが伝わることが第一条件であるが，T細胞表面のCD28が，抗原提示細胞のCD80あるいはCD86分子と結合し，第二のシグナルを伝達することが重要であることが明らかになってきた(図6)。さらに，CD80やCD86と結合して活性化したT細胞にはCTLA-4が発現し，CD28と強く結合してT細胞の活性化を抑制することがわかってきた。CTLA-4断片を持つ**Abatacept**は，抗原提示細胞のCD80/86分子とT細胞のCD28が結合することを阻害することによって，T細胞の活性化を抑制する。**Abatacept**は，2005年メトトレキサートやTNF-α阻害薬で効果不十分な関節リウマチ治療薬として米国で承認された。本邦では第I相試験中である。

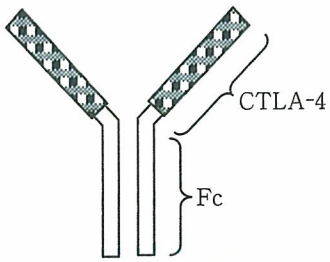

図8　Abataceptの構造(日本未承認)

おわりに

今回は，免疫機能に関わるタンパク質性医薬品を取り上げ，それらの名前の由来と作用機構を紹介した。例えば，炎症性サイトカインTNF-αの作用をブロックする医薬品として紹介した**インフリキシマブ**および**アダリムマブ**は，抗TNF-α抗体としてTNF-αが細胞表面受容体に結合することを阻害する。また，**エタネルセプト**はTNF-α受容体様分子としてTNF-αとその受容体の結合を阻害する。一方，他の受容体様分子**Alefacept**はLFA-3様分子(CD2受容体)として，また**Abatacept**はCTLA-4様分子(CD80/86受容体)としてT細胞や抗原提示細胞に結合し，TNF-αの放出を抑制する。これらの医薬品の構造遺伝子の由来と作用機構はまったく異なるが，ステムからそれらを容易に推測することができる。

以上，生物薬品のステムの2回目として，モノクローナル抗体のステム「**-mab**」および受容体分子のステム「**-cept**」について紹介した。

■参考文献
本稿作成に使用した参考文献は，本連載第5回(本誌2006年12月号)に記載した。また，新見伸吾，原島 瑞，川西 徹，早川堯夫：抗体医薬の現状と展望，医薬品研究，36，163-193(2005)も参考にした。

Journal of Cellular Physiology

Granulocyte Colony-Stimulating Factor Promotes the Translocation of Protein Kinase Cι in Neutrophilic Differentiation Cells

TOSHIE KANAYASU-TOYODA,[1] TAKAYOSHI SUZUKI,[1] TADASHI OSHIZAWA,[1] ERIKO UCHIDA,[2] TAKAO HAYAKAWA,[2] AND TERUHIDE YAMAGUCHI[1]*

[1]*Division of Cellular and Gene Therapy Products, National Institute of Health Sciences, Tokyo, Japan*

[2]*National Institute of Health Sciences, Tokyo, Japan*

Previously, we suggested that the phosphatidylinositol 3-kinase (PI3K)-p70 S6 kinase (p70 S6K) pathway plays an important role in granulocyte colony-stimulating factor (G-CSF)-dependent enhancement of the neutrophilic differentiation and proliferation of HL-60 cells. While atypical protein kinase C (PKC) has been reported to be a regulator of p70 S6K, abundant expression of PKCι was observed in myeloid and lymphoid cells. Therefore, we analyzed the participation of PKCι in G-CSF-dependent proliferation. The maximum stimulation of PKCι was observed from 15 to 30 min after the addition of G-CSF. From 5 to 15 min into this lag time, PKCι was found to translocate from the nucleus to the membrane. At 30 min it re-translocated to the cytosol. This dynamic translocation of PKCι was also observed in G-CSF-stimulated myeloperoxidase-positive cells differentiated from cord blood cells. Small interfering RNA for PKCι inhibited G-CSF-induced proliferation and the promotion of neutrophilic differentiation of HL-60 cells. These data indicate that the G-CSF-induced dynamic translocation and activation processes of PKCι are important to neutrophilic proliferation.

J. Cell. Physiol. 211: 189–196, 2007.

Hematopoietic cell differentiation is regulated by a complex network of growth and differentiation factors (Tenen et al., 1997; Ward et al., 2000). Granulocyte colony-stimulating factor (G-CSF) and its receptors are pivotal to the differentiation of myeloid precursors into mature granulocytes. In previous studies (Kanayasu-Toyoda et al., 2002) on the neutrophilic differentiation of HL-60 cells treated with either dimethyl sulfoxide (DMSO) or retinoic acid (RA), heterogeneous transferrin receptor (Trf-R) populations—transferrin receptor-positive (Trf-R^+) cells and transferrin receptor-negative (Trf-R^-) cells—appeared 2 days after the addition of DMSO or RA. The Trf-R^+ cells were proliferative-type cells that had higher enzyme activity of phosphatidylinositol 3-kinase (PI3K) and protein 70 S6 kinase (p70 S6K), whereas the Trf-R^- cells were differentiation-type cells of which Tyr705 in STAT3 was much more phosphorylated by G-CSF. Inhibition of either PI3K by wortmannin or p70 S6K by rapamycin was found to eliminate the difference in differentiation and proliferation abilities between Trf-R^+ and Trf-R^- cells in the presence of G-CSF (Kanayasu-Toyoda et al., 2002). From these results, we concluded that proteins PI3K and p70 S6K play important roles in the growth of HL-60 cells and negatively regulate neutrophilic differentiation. On the other hand, the maximum kinase activity of PI3K was observed at 5 min after the addition of G-CSF (Kanayasu-Toyoda et al., 2002) and that of p70 S6K was observed between 30 and 60 min after, indicating a lag time between PI3K and p70 S6K activation. It is conceivable that any signal molecule(s) must transduce the G-CSF signal during the time lag between PI3K and p70 S6K. Chung et al. (1994) also showed a lag time between PI3K and p70 S6K activation on HepG2 cells stimulated by platelet-derived growth factor (PDGF), suggesting that some signaling molecules also may transduce between PI3K and p70S6K.

Protein kinase C (PKC) is a family of Ser/Thr kinases involved in the signal transduction pathways that are triggered by numerous extracellular and intracellular stimuli. The PKC family has been shown to play an essential role in cellular functions, including mitogenic signaling, cytoskeleton rearrangement, glucose metabolism, differentiation, and the regulation of cell survival and apoptosis. Eleven different members of the PKC family have been identified so far. Based on their structural similarities and cofactor requirements, they have been grouped into three subfamilies: (1) the classical or conventional PKCs (cPKCα, β_1, β_2, and γ), activated by Ca^{2+}, diacylglycerol, and phosphatidyl-serine; (2) the novel PKCs (nPKCδ, ε, η, and θ), which are independent of Ca^{2+} but still responsive to diacylglycerol; and (3) the atypical PKCs (aPKCζ and ι/λ), where PKCλ is the homologue of human PKCι. Atypical PKCs differ significantly from all other PKC family

Abbreviations: DMSO, dimethyl sulfoxide; fMLP-R, formyl-Met-Leu-Phe receptor; RA, retinoic acid; G-CSF, granulocyte colony-stimulating factor; Trf-R, transferrin receptor; BSA, bovine serum albumin; FITC, fluorescein isothiocyanate; PBS, phosphate-buffered saline; PKC, protein kinase C; PI3K, phosphatidylinositol 3-kinase; p70 S6K, protein 70 S6 kinase; SDS–PAGE, sodium dodecyl sulfate-polyacrylamide gel electrophoresis; siRNA, small interfering RNA; PMN, polymorphonuclear leukocyte.

Contract grant sponsor: Ministry of Health, Labor, and Welfare of Japan.
Contract grant sponsor: Ministry of Education, Culture, Sports, Science, and Technology of Japan.

*Correspondence to: Teruhide Yamaguchi, Division of Cellular and Gene Therapy Products, National Institute of Health Sciences, 1-18-1, Kamiyoga, Setagaya-ku, Tokyo 158-8501, Japan.
E-mail: yamaguch@nihs.go.jp

Received 31 May 2006; Accepted 22 September 2006

Published online in Wiley InterScience (www.interscience.wiley.com.), 28 November 2006.
DOI: 10.1002/jcp.20930

members in their regulatory domains, in that they lack both the calcium-binding domain and one of the two zinc finger motifs required for diacylglycerol binding (Liu and Heckman, 1998). Romanelli et al. (1999) reported that p70 S6K is regulated by PKCζ and participates in a PI3K-regulated signaling complex. On the other hand, Selbie et al. (1993) reported that the tissue distribution of PKCζ is different from that of PKCι/λ, and that PKCι/λ appears to be widely expressed. If the p70 S6K could be activated by aPKC, the regulation of p70 S6K activation would seem to depend on the tissue-specific expression of PKCι and/or PKCζ. In neutrophilic lineage cells, the question is which aPKC participates in the regulation of p70 S6K on G-CSF signaling.

In this study, we show that G-CSF activated PKCι, promoting its translocation from the nucleus to the cell surface membrane and subsequently to the cytosol in DMSO-treated HL-60 cells. We also show the translocation of PKCι using myeloperoxidase-positive neutrophilic lineage differentiated from cord blood, which is a rich source of immature myeloid cells (Fritsch et al., 1993; Rappold et al., 1997; Huang et al., 1999; Debili et al., 2001; Hao et al., 2001). We concluded that PKCι translocation and activation by G-CSF are needed for neutrophilic proliferation.

Materials and Methods

Reagents

Anti-p70 S6K polyclonal antibody was obtained from Santa Cruz Biotechnology (Santa Cruz, CA). Anti-PKCι polyclonal antibody and monoclonal antibody were purchased from Santa Cruz Biotechnology and from Transduction Laboratories (Lexington, KY), respectively. Anti-PKCζ polyclonal antibody was purchased from Cell Signaling Technology (Beverly, MA). Anti-myeloperoxidase antibody was purchased from Serotec Ltd. (Oxford, UK). GF 109203X, and Gö 6983 were obtained from Calbiochem-Novabiochem (San Diego, CA). Wortmannin was obtained from Sigma Chemical (St. Louis, MO). Anti-Histon-H1 antibody, anti-Fcγ receptor IIa (CD32) antibody, and anti-lactate dehydrogenase antibody were from Upstate Cell Signaling Solutions (Lake Placid, NY), Lab Vision Corp. (Fremont, CA), and Chemicon International, Inc. (Temecula, CA), respectively.

Cell culture

HL-60, Jurkut, K562, U937, and THP-1 cells were kindly supplied by the Japanese Collection of Research Bioresources Cell Bank (Osaka, Japan). Cells were maintained in RPMI 1640 medium containing 10% heat-inactivated FBS and 30 mg/L kanamycin sulfate at 37°C in moisturized air containing 5% CO_2. The HL-60 cells, which were at a density of 2.5×10^5 cells/ml, were differentiated by 1.25% DMSO. Two days after the addition of DMSO, the G-CSF-induced signal transduction was analyzed using either magnetically sorted cells or non-sorted cells.

Magnetic cell sorting

To prepare Trf-R^- and Trf-R^+ cells, magnetic cell sorting was performed as previously reported (Kanayasu-Toyoda et al., 2002), using an automatic cell sorter (AUTO MACS; Miltenyi Biotec, Bergisch Gladbach, Germany). After cell sorting, both cell types were used for Western blotting and PKCι enzyme activity analyses.

Preparation of cell lysates and immunoblotting

For analysis of PKCι and PKCζ expression, a PVDF membrane blotted with 50 μg of various tissues per lane was purchased from BioChain Institute (Hayward, CA). Both a polymorphonuclear leukocytes (PMNs) fraction and a fraction containing lymphocytes and monocytes were isolated by centrifugation (400*g*, 25 min) using a Mono-poly resolving medium (Dai-Nippon Pharmaceutical, Osaka, Japan) from human whole blood, which was obtained from a healthy volunteer with informed consent. T-lymphocytes were further isolated from the mixture fraction using the Pan T Cell Isolation Kit (Miltenyi Biotec) according to the manufacturer's protocol. T-lymphocytes, PMNs, HL-60 cells, Jurkut cells, K562 cells, and U937 cells (1×10^7) were collected and lysed in lysis buffer containing 1% Triton X-100, 10 mM K_2HPO_4/KH_2PO_4 (pH 7.5), 1 mM EDTA, 5 mM EGTA, 10 mM $MgCl_2$, and 50 mM β-glycerophosphate, along with 1/100 (v/v) protease inhibitor cocktail (Sigma Chemical) and 1/100 (v/v) phosphatase inhibitor cocktail (Sigma Chemical). The cellular lysate of 10^6 cells per lane was subjected to Western blotting analysis. Human cord blood was kindly supplied from the Metro Tokyo Red Cross Cord Blood Bank (Tokyo, Japan) with informed consent. Mononuclear cells, isolated with the Lymphoprep™ Tube (Axis-Shield PoC AS, Oslo, Norway), were cultured in RPMI 1640 medium containing 10% FBS in the presence of G-CSF for 3 days. Cultured cells were collected, and the cell lysate was subjected to Western blotting analysis.

A fraction of the plasma membrane, cytosol, and nucleus of the DMSO-treated HL-60 cells was prepared by differential centrifugation after the addition of G-CSF, as described previously (Yamaguchi et al., 1999). After the cells that had been suspended in 250 mM sucrose/10 mM Tris-HCl (pH 7.4) containing 1/100 (v/v) protease inhibitor cocktail (Sigma Chemical) were gently disrupted by freezing and thawing, they were centrifuged at 800*g*, 4°C for 10 min. The precipitation was suspended in 10 mM Tris-HCl (pH 6.7) supplemented with 1% SDS. It was then digested by benzon nuclease at 4°C for 1 h and used as a sample of the nuclear fraction. After the post-nucleus supernatant was re-centrifuged at 100,000 rpm (452,000*g*) at a temperature of 4°C for 40 min, the precipitate was used as a crude membrane fraction and the supernatant as a cytosol fraction. Western blotting analysis was then performed as described previously (Kanayasu-Toyoda et al., 2002). The bands that appeared on x-ray films were scanned, and the density of each band was quantitated by Scion Image (Scion, Frederick, MD) using the data from three separate experiments.

Kinase assay

The activity of PKCι was determined by phosphorous incorporation into the fluorescence-labeled pseudosubstrate (Pierce Biotechnology, Rockford, IL). The cell lysates were prepared as described above and immunoprecipitated with the anti-PKCι antibody. Kinase activity was measured according to the manufacturer's protocol. In the analysis of inhibitors effects, cells were pretreated with a PI3K inhibitor, wortmannin (100 nM), or PKC inhibitors, GF109207X (10 μM) and Gö6983 (10 μM) for 30 min, and then stimulated by G-CSF for 15 min.

Observation of confocal laser-scanning microscopy

Upon the addition of G-CSF, PKCι localization in the DMSO-treated HL-60 cells for 2 days was examined by confocal laser-activated microscopy (LSM 510, Carl Zeiss, Oberkochen, Germany). The cells were treated with 50 ng/ml G-CSF for the indicated periods and then fixed with an equal volume of 4.0% paraformaldehyde in PBS(−). After treatment with ethanol, the fixed cells were labeled with anti-PKCι antibody and with secondary antibody conjugated with horseradish peroxidase. They were then visualized with TSA™ Fluorescence Systems (PerkinElmer, Boston, MA).

Mononuclear cells prepared from cord blood cells were cultured in RPMI 1640 medium containing 10% FBS in the presence of G-CSF for 7 days. Then, for serum and G-CSF starvation, cells were cultured in RPMI 1640 medium containing 1% BSA for 11 h. After stimulation by 50 ng/ml G-CSF, the cells were fixed, stained with both anti-PKCι polyclonal antibody and anti-myeloperoxidase monoclonal antibody, and finally visualized with rhodamine-conjugated anti-rabbit IgG and FITC-conjugated anti-mouse IgG, respectively.

RNA interference

Two pairs of siRNAs were chemically synthesized: annealed (Dharmacon RNA Technologies, Lafayette, CO) and transfected into HL-60 cells using Nucleofector™ (Amaxa, Cologne, Germany). The sequences of sense siRNAs were as follows: PKCι, GAAGAAGCCUUUAGACUUUTA; p70 S6K, GCAAGGAGUCUAUCCAUGAUU. As a control, the sequence ACUCUAUCGCCAGCGUGACUU was used. Forty-eight hours after treatment with siRNA, the cells were lysed for Western blot analysis. For proliferation and differentiation assay, cells were transfected with siRNA on the first day, treated with DMSO on the second day, and supplemented with G-CSF on the third day. After cells were subsequently cultured for 5 days, cell numbers and formyl-Met-Leu-Phe receptor (fMLP-R) expression were determined.

fMLP-R expression

The differentiated cells were collected and incubated with FITC-conjugated fMLP; then, labeled cells were subjected to flow cytometric analysis (FACSCalibur, Becton Dickinson, Franklin Lakes, NJ).

Statistical analysis

Statistical analysis was performed using unpaired Student's *t*-test. Values of $P < 0.05$ were considered to indicate statistical significance. Each experiment was repeated at least three times and representative data were indicated.

Results

The distribution of atypical PKC in various tissues and cells

Previously, we reported that the PI3K-p70 S6K-cMyc pathway plays an important role in the G-CSF-induced proliferation of DMSO-treated HL-60 cells, not only by enhancing the activity of both PI3K and p70 S6K but also by inducing the c-Myc protein (Kanayasu-Toyoda et al., 2002, 2003). We also reported that G-CSF did not stimulate Erk1, Erk2, or 4E-binding protein 1. The maximum kinase activity of PI3K was observed 5 min after the addition of G-CSF, and that of p70 S6K was observed between 30 and 60 min after. It is conceivable that any signal molecule(s) must transduce the G-CSF signal during the time lag between PI3K and p70 S6K. Romanelli et al. (1999) suggested that the activation of p70 S6K is regulated by PKCξ and participates in the PI3K-regulated signaling complex. To examine the role of atypical PKC in the G-CSF-dependent activation and the relationship between atypical PKC and p70 S6K, the protein expression of PKCζ and PKCι in various human tissues and cells was analyzed by Western blotting. As shown in Figure 1A, both of the atypical PKCs were markedly expressed in lung and kidney but were weakly expressed in spleen, stomach, and placenta. In brain, cervix, and uterus, the expression of only PKCι was observed. Selbie et al. (1993) have reported observing the expression of PKCζ not in protein levels but in RNA levels, in the kidney, brain, lung, and testis, and that of PKCι in the kidney, brain, and lung. In this study, the protein expression of PKCι in the kidney, brain, and lung was consistent with the RNA expression of PKCι. Despite the strong expression of PKCζ RNA in brain (Selbie et al., 1993), PKCζ protein was scarcely observed. Although PKCι proteins were scarcely expressed in neutrophils and T-lymphocytes in peripheral blood, they were abundantly expressed in immature blood cell lines, that is, Jurkut, K562, U937, and HL-60 cells (Fig. 1B), in contrast with the very low expression of PKCζ proteins. In mononuclear cells isolated from umbilical cord blood, which contains large numbers of immature myeloid cells and has a high proliferation ability, the expression of PKCι proteins was also observed. Since Nguyen and Dessauer (2005) have reported observing abundant PKCζ proteins in THP-1 cells, as a positive control for PKCζ, we also performed a Western blot of THP-1 cells (Fig. 1B, right part). While PKCι was markedly expressed in both THP-1 and HL-60 cells, PKCζ was observed only in THP-1 cells.

These data suggested that PKCζ and PKCι were distributed differently in various tissues and cells, and that mainly PKCι proteins were expressed in proliferating blood cells.

Stimulation of PKCι activity by G-CSF

Among the 11 different members of the PKC family, the aPKCs (ζ and ι/λ) have been reported to activate p70 S6K activity and to be regulated by PI3K (Akimoto et al., 1998; Romanelli et al., 1999). As shown in Figure 1, although the PKCζ proteins were not detected by Western blotting in HL-60 cells or mononuclear cells isolated from cord blood cells, it is possible that PKCι could functionally regulate p70 S6K as an upstream

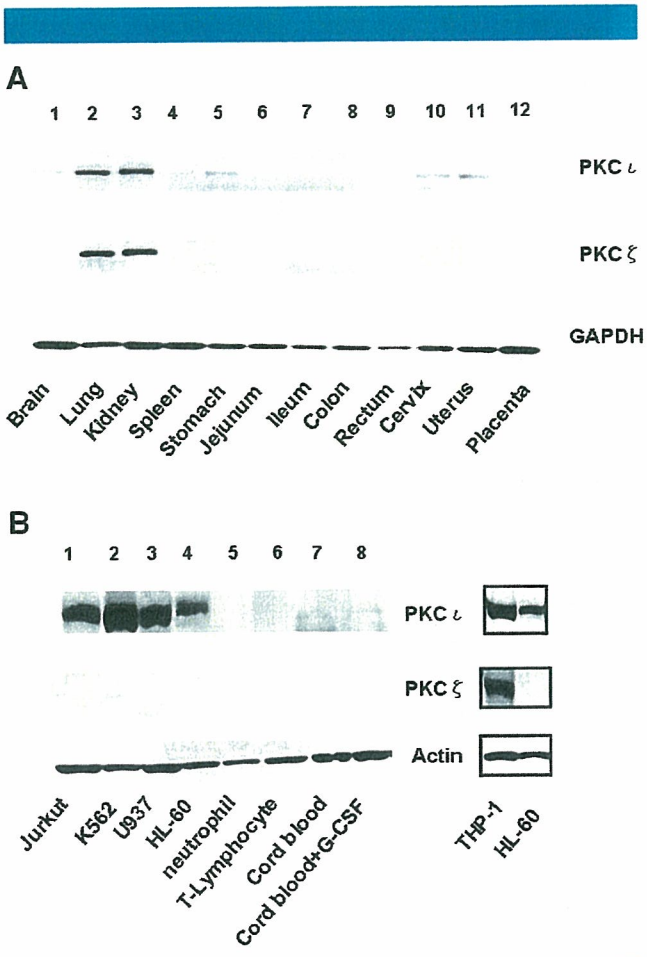

Fig. 1. Different distributions of PKCζ and PKCι. The protein expression of PKCι appears in the upper part and that of PKCζ in the middle part in various tissues and cells. A: 1, brain; 2, lung; 3, kidney, 4, spleen; 5, stomach; 6, jejunum; 7, ileum; 8, colon; 9, rectum; 10, cervix; 11, uterus; 12, placenta. Anti-GAPDH blot is a control for various tissues. B: 1, jurkut cells; 2, K562 cells; 3, U937 cells; 4, HL-60 cells; 5, neutrophils; 6, T-lymphocytes; 7, mononuclear cells from cord blood in the absence of G-CSF; 8, mononuclear cells from cord blood in the presence of G-CSF. Anti-actin blot is a control. The right part shows immunoblots of PKCι, PKCζ, and actin of THP-1 cells as a positive control for PKCζ. The cell numbers of THP-1 and HL-60 cells were adjusted in relation to other cells on the left parts.

regulator in these cells. Therefore, we focused on the role of PKCι as the possible upstream regulator of p70 S6K in neutrophil lineage cells. First, we compared the expression of PKCι in both Trf-R^+ and Trf-R^- cells. PKCι proteins were expressed more abundantly in Trf-R^+ cells than in Trf-R^- cells (Fig. 2A, middle part), as with the p70 S6K proteins. A time course study of PKCι activity upon the addition of G-CSF revealed the maximum stimulation at 15 min, lasting until 30 min. The G-CSF-dependent activation of PKCι was inhibited by the PKC inhibitors wortmannin, GF 109203X, and Gő 6983. Considering the marked inhibitory effect of wortmannin on PKCι and evidence that the maximum stimulation of PI3K was observed at 5 min after the addition of G-CSF, PI3K was determined to be the upstream regulator of PKCι in the G-CSF signal transduction of HL-60 cells. The basal activity of PKCι in Trf-R^+ cells was higher than that in Trf-R^- cells, and G-CSF was more augmented. In Trf-R^- cells, PKCι activity was scarcely stimulated by G-CSF. This tendency of PKCι to be activated by G-CSF was similar to that of PI3K (Kanayasu-Toyoda et al., 2002).

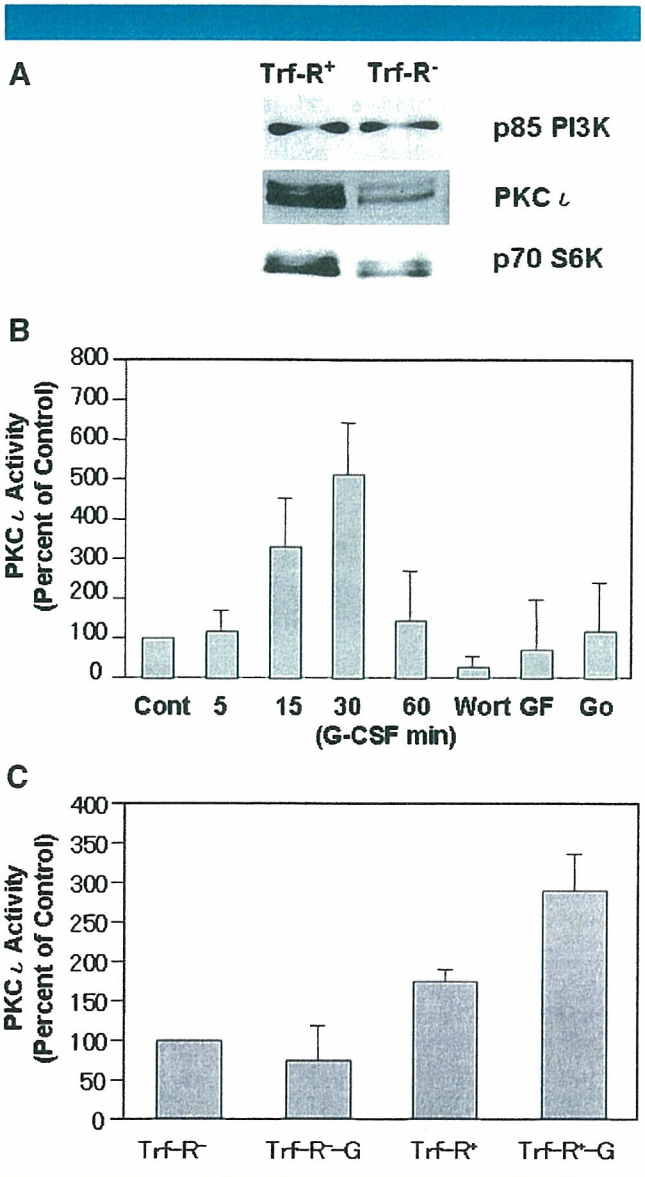

Fig. 2. Expression of PKCι in Trf-R$^+$ and Trf-R$^-$ cells and effects of G-CSF on PKCι activity. A: The expression of PKCι in Trf-R$^+$ and Trf-R$^-$ cells was subjected to Western blot analysis after magnetic cell sorting. B: The G-CSF-dependent PKCι activation of the DMSO-treated HL-60 cells was measured. The x-axis represents the time lapse (min) after the G-CSF stimulation and the y-axis percent of control that was not stimulated by G-CSF. Columns and bars represent the mean ± SD, using data from three separate experiments. Wort: wortmannin (100 nM), GF: GF109207X (10 μM), Gö: Gö6983 (10 μM). Cells were pretreated with each inhibitor and then stimulated by G-CSF for 15 min. C: The PKCι activity in the Trf-R$^+$ and Trf-R$^-$ cells 30 min after the addition of G-CSF. The y-axis represents the percentage of control that was non-stimulated Trf-R$^-$ cells. Columns and bars represent the mean ± SD, using data from three separate experiments.

Effects of G-CSF on PKCι translocation

Muscella et al. (2003) demonstrated that the translocation of PKCζ from the cytosol to the nucleus or membrane is required for c-Fos synthesis induced by angiotensin II in MCF-7 cells. It was also reported that high glucose induced the translocation of PKCι (Chuang et al., 2003). These results suggest that the translocation of aPKC plays an important role in its signaling. To clarify the translocation of PKCι, immuno-histochemical staining (Fig. 3) and biochemical fractionation (Fig. 4) in DMSO-induced HL-60 cells were performed after the addition of G-CSF. In a non-stimulated condition, PKCι in the HL-60 cells treated with DMSO for 2 days (Fig. 3, control) was detected mainly in the nucleus. Analysis of Western blotting (Fig. 4, left parts) and quantification of the bands (Fig. 4, right columns) also revealed that PKCι was localized and observed mainly in the nuclear fraction (Fig. 4A). During the 5–15 min period after the addition of G-CSF, PKCι was found to translocate (Figs. 3 and 4B) into the membrane fraction, after which it re-translocated into the cytosol fraction (Fig. 4C). In the presence of wortmannin, the G-CSF-induced translocation of PKCι into the plasma membrane failed, but PKCι was found to localize in the cytosolic fraction (Figs. 3 and 4B). Myeloperoxidase is thought to be expressed in stage from promyelocytes to mature neutrophils (Manz et al., 2002). In human cord blood cells (Fig. 3), PKCι in the cells co-stained with anti-myeloperoxidase antibody was also localized in the nucleus after serum depletion (Fig. 3B top parts). Ten minutes after the addition of G-CSF, PKCι was found to translocate into the membrane, and then into the cytosol at 30 min after the addition of G-CSF. In the presence of wortmannin, the G-CSF-induced translocation of PKCι into the plasma membrane failed but PKCι was found to localize in the cytosol. This suggested that the dynamic translocation of PKCι induced by G-CSF is a universal phenomenon in neutrophilic lineage cells. Taken together, these data support the possibility that PI3K plays not only an important role upstream of PKCι but also triggers the translocation from nucleus to membrane upon the addition of G-CSF.

In order to assess the purity of each cellular fraction, antibodies against specific markers were blotted. As specific markers, Histon-H1, Fcγ receptor IIa (CD32), and lactate dehydrogenase (LDH) were used for the nuclear, membrane, and cytosolic fractions, respectively. The purities of the nuclear, membrane, and cytosolic fractions were 82.0, 78.5, and 72.2%, respectively (Fig. 4D).

Effects of siRNA for PKCι on proliferation and differentiation

To determine the role of PKCι in neutrophilic proliferation and differentiation, PKCι was knocked down by siRNA. When the protein level of PKCι was specifically downregulated by siRNA for PKCι (Fig. 5A), G-CSF failed to enhance proliferation of the cells during 5 days' cultivation (Fig. 5B). The effect of siRNA for PKCι on neutrophilic differentiation in terms of fMLP-R expression was also determined. As shown in Figure 5C, fMLP-R expression was promoted by siRNA for PKCι in either the presence (lower part) or absence (upper part) of G-CSF. These data indicate that PKCι positively regulates G-CSF-induced proliferation and negatively regulates the differentiation of DMSO-treated HL-60 cells.

Discussion

We previously reported that PI3K/p70 S6K plays an important role in the regulation of the neutrophilic differentiation and proliferation of HL-60 cells. Akimoto et al. (1998) and Romanelli et al. (1999) reported that p70 S6K is regulated by aPKC and aPKCλ/PKCζ, respectively. At first, we showed that the distribution of PKCζ and PKCι proteins in various human tissues and cells was not similar (Fig. 1A), and that PKCι are more abundantly expressed in proliferating blood cells: Jurkut, K562, U937, and HL-60 cells (Fig. 1B). Moreover, PKCι proteins were also observed in cultured mononuclear cells of cord blood, in which the myeloid progenitors were enriched in the presence or absence of G-CSF (Fig. 1B). The myeloperoxidase-positive cells as neutrophilic lineage cells, a myeloid marker, were also stained with the antibody of PKCι (Fig. 3B). Although PKCζ proteins are barely detected in

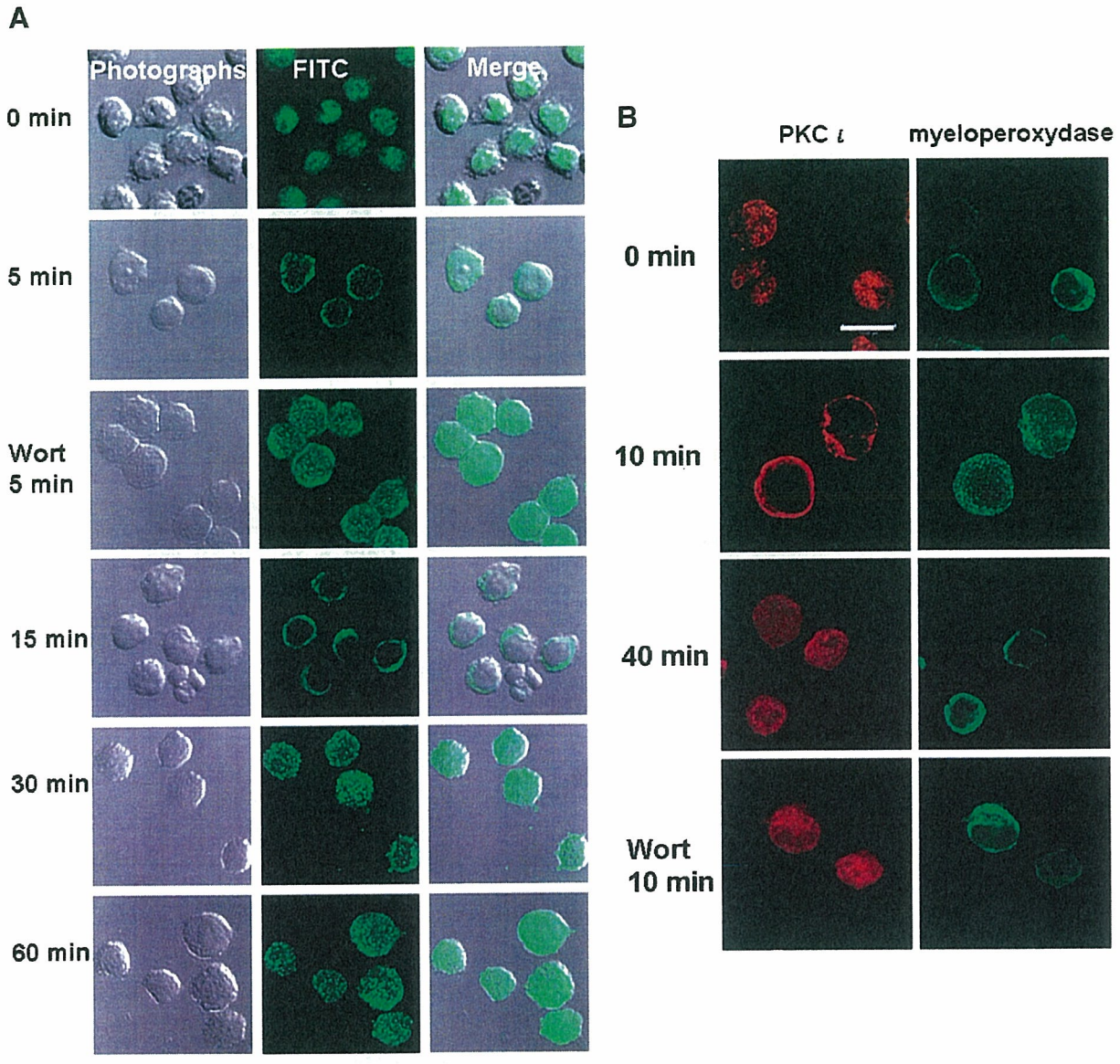

Fig. 3. Translocation of PKCι after the activation of G-CSF. A: 2 days after the addition of DMSO, HL-60 cells stimulated by G-CSF were fixed, incubated with anti-PKCι antibody, and visualized as described above. The photographs can be seen at the left part of the figure, the fluorescent photographs in the middle of the figure, and the merged images at the right. B: G-CSF-stimulated mononuclear cells from cord blood were stained with anti-PKCι antibody (red, left part) and anti-myeloperoxidase antibody (green, right part) after serum depletion. Under no stimulation, PKCι was observed in the nucleus. G-CSF promoted the translocation of PKCι to the membrane within 5–15 min, and then to the cytosol. Wort: wortmannin. White bar: 10 μm.

neutrophilic HL-60 cells, PKCι proteins were markedly expressed in these cells (Fig. 1B). This study showed, for the first time, the stimulation of PKCι activity in G-CSF-treated HL-60 cells (Fig. 2B) at 15–30 min after the addition of G-CSF. Maximum activation from the addition of NGF in PC12 cells was also observed at 15 min (Wooten et al., 2001).

Atypical PKCs are lipid-regulated kinases that need to be localized to the membrane in order to be activated. PKCζ is directly activated by phosphatidylinositol 3,4,5-trisphosphate, a product of PI3K (Nakanishi et al., 1993). We previously reported that the maximum activation of PI3K was observed in HL-60 cells 5 min after the addition of G-CSF (Kanayasu-Toyoda et al., 2002). Most investigators have reported the translocation of aPKC in either muscle cells or adipocytes stimulated by insulin (Andjelkovic et al., 1997; Goransson et al., 1998; Galetic et al., 1999; Standaert et al., 1999; Braiman et al., 2001; Chen et al., 2003; Kanzaki et al., 2004; Sasaoka et al., 2004; Herr et al., 2005). In response to insulin stimulation, aPKCζ/λ is translocated to the plasma membrane (Standaert et al., 1999; Braiman et al., 2001), where aPKCζ/λ is believed to be activated (Galetic et al., 1999; Kanzaki et al., 2004). In the present study, the addition of G-CSF induced PKCι to translocate to the membrane from the nucleus within 5–15 min (Figs. 3 and 4), and this translocation to the plasma membrane accompanied the full activation of PKCι (Fig. 2B). Previously we reported also that the maximum activation of p70 S6K in HL-60 cells was observed from 30 to 60 min after the addition of G-CSF (Kanayasu-Toyoda et al., 1999, 2002), suggesting that there was a time lag between the activation of PI3K and p70 S6K upon the addition of G-CSF in HL-60 cells. In the present study, PKCι was

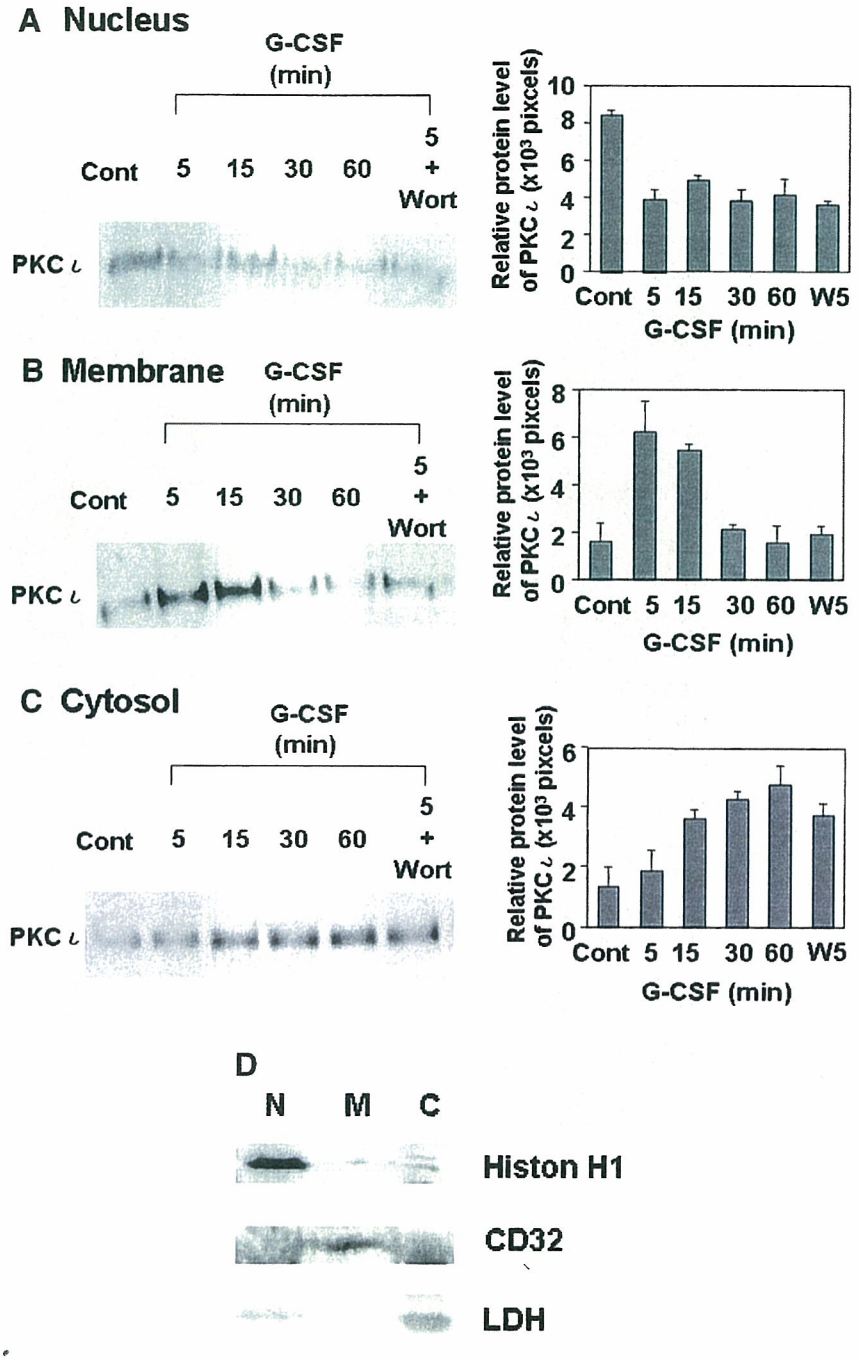

Fig. 4. Translocation of PKCι after activation by G-CSF on biochemical fractionation. The cells were differentiated as described in the Figure 3 legend. After stimulation by G-CSF, the amounts of PKCι proteins in the nucleus (A), plasma membrane (B), and cytosol (C), as fractionated by differential centrifugation, were analyzed by Western blotting (left parts). The right parts show the quantitation of the bands of PKCι proteins. Wort or W: wortmannin. PKCι protein was quantitated using data from three separate experiments. Columns and bars represent the mean ± SD. D: Each cell fraction was immunoblotted with antibodies of specific marker. Histon-H1, Fcγ receptor IIa (CD32), and lactate dehydrogenase (LDH) are specific markers for nuclear (N), membrane (M), and cytosolic (C) fractions, respectively.

found to re-translocate from the plasma membrane to the cytosol (Figs. 3 and 4C). In the presence of wortmannin, an inhibitor of PI3K, PKCι failed to translocate into the plasma membrane, but instead translocated to cytosol directly from the nucleus upon the addition of G-CSF (Figs. 3 and 4B). PKCι translocation was also observed in myeloperoxidase-positive cells derived from human cord blood (Fig. 3B), indicating that G-CSF-induced dynamic translocation of PKCι occurred in not only a limited cell line but also neutrophilic lineage cells. These data suggest that PI3K plays an important role in the activation and translocation of PKCι during the G-CSF-induced activation of myeloid cells. Furthermore, the translocation to the plasma membrane in response to G-CSF is wortmannin sensitive, but the translocation from the nucleus upon G-CSF stimulation is not affected by wortmannin, suggesting that the initial signal of G-CSF-induced PKCι translocation from the nucleus may be

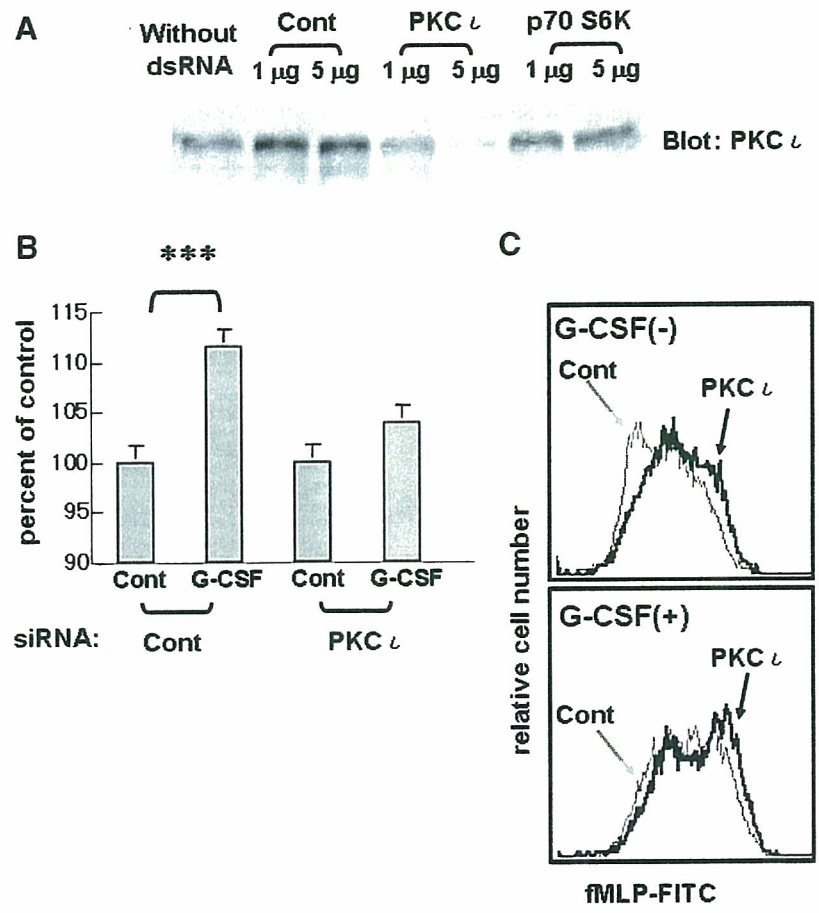

Fig. 5. Effects of siRNA of PKCι on proliferation, differentiation, and phosphorylation at various sites of p70 S6K. A: Forty-eight hours after transfection with siRNA of PKCι or p70 S6K, protein levels of PKCι were compared. B: Proliferation of the cells transfected with siRNA of PKCι or control (Cont) was measured 5 days after the addition of G-CSF. Columns and bars represent the mean ± SD of triplicate wells (*$P < 0.001$). C: fMLP-R expression was analyzed by flow cytometry 5 days after the addition of G-CSF. The gray arrow indicates cells transfected with the control sequence of double-stranded RNA (Cont, gray lines), and the black arrow the cells transfected with siRNA for PKCι (black lines) in the presence (lower part) or absence (upper part) of G-CSF.**

PI3K-independent, but association of PKCι with the plasma membrane could be mediated through a PI3K-dependent signal. Cord blood is an important material of blood transplantation for leukemia (Bradstock et al., 2006; Ooi, 2006; Yamada et al., 2006) or for congenital neutropenia (Mino et al., 2004; Nakazawa et al., 2004) because it contains many hematopoietic stem cells such as CD34-positive cells or CD133-positive cells, and also contains immature granulocytes. The neutrophilic differentiation and proliferation are necessary processes after transplantation.

Formyl-Met-Leu-Phe peptide evokes the migration, superoxide production, and phagocytosis of neutrophils through fMLP-R, a suitable marker for neutrophilic differentiation. In this study, the reduction of PKCι by siRNA inhibited G-CSF-induced proliferation (Fig. 5B) and promoted neutrophilic differentiation (Fig. 5C) in terms of fMLP-R expression. These data, however, suggest that PKCι promoted G-CSF-induced proliferation and blocked differentiation at the same time.

The substrates of aPKC have recently been reported: namely, the cytoskeletal protein Lethal giant larvae (Lgl) was phosphorylated by Drosophila aPKC (Betschinger et al., 2003) and glyceraldehydes-3-phosphate dehydrogenase (GAPDH) was phosphorylated by PKCι (Tisdale, 2002) directly in both cases. While the direct phosphorylation of p70 S6K by aPKC was not observed (Akimoto et al., 1998; Romanelli et al., 1999), the enzyme activity of p70 S6K was markedly enhanced by co-transfection with aPKC and PDK-1, the latter of which is recruited to the membrane due to the binding of phosphatidylinositol-3,4,5-trisphosphate to its PH domain (Anderson et al., 1998). The addition of G-CSF induced PKCι to increase phosphorylation at Thr-389, which is the site most closely related to enzyme activity among the multi-phosphorylation sites of p70 S6K (Weng et al., 1998). However, the mammalian target of rapamycin (mTOR), an upstream regulator, also phosphorylates Thr-389 of p70 S6K and markedly stimulates p70 S6K activity under coexistence with PDK-1 (Isotani et al., 1999). We could not rule out the possibility that other PKC isoforms can contribute to the activation of p70 S6K. We postulated that in G-CSF-stimulated HL-60 cells, PKCι contributes to p70 S6K activation as an upstream regulator.

Atypical PKC isoforms are reported to play an important role in the activation of IκB kinase β (Lallena et al., 1999). In PKCζ-deficient mice, impaired signaling through the B-cell receptor resulted in the inhibition of cell proliferation and survival while also causing defects in the activation of ERK and the transcription of NF-κB-dependent genes (Martin et al., 2002). Moreover, Lafuente et al. (2003) demonstrated that the loss of Par-4, that is, the genetic inactivation of the aPKC inhibitor, led to an increased proliferative response of

peripheral T cells when challenged through the T-cell receptor. However, it has been reported that PKCλ-deficient mice have a lethal phenotype at the early embryonic stage (Soloff et al., 2004). Based on the present results and those of previous reports (Kanayasu-Toyoda et al., 1999, 2002), we postulate that PKCι plays an important role in regulating G-CSF-induced proliferation in neutrophilic lineage cells.

Acknowledgments

We thank the Metro Tokyo Red Cross Cord Blood Bank (Tokyo, Japan) for their kind cooperation. This work was supported in part by a grand-in-aid for health and labor science research (H17-SAISEI-021) from the Japanese Ministry of Health, Labor and Welfare, and in part by a grand-in-aid for Research on Health Sciences focusing on Drug Innovation from the Japan Health Sciences Foundation.

Literature Cited

Akimoto K, Nakaya M, Yamanaka T, Tanaka J, Matsuda S, Weng QP, Avruch J, Ohno S. 1998. Atypical protein kinase Clambda binds and regulates p70 S6 kinase. Biochem J 335:417–424.

Anderson KE, Coadwell J, Stephens LR, Hawkins PT. 1998. Translocation of PDK-1 to the plasma membrane is important in allowing PDK-1 to activate protein kinase B. Curr Biol 8:684–691.

Andjelkovic M, Alessi DR, Meier R, Fernandez A, Lamb NJ, Frech M, Cron P, Cohen P, Lucocq JM, Hemmings BA. 1997. Role of translocation in the activation and function of protein kinase B. J Biol Chem 272:31515–31524.

Betschinger J, Mechtler K, Knoblich JA. 2003. The Par complex directs asymmetric cell division by phosphorylating the cytoskeletal protein Lgl. Nature 422:326–330.

Bradstock KF, Hertzberg MS, Kerridge IH, Svennilson J, McGurgan M, Huang G, Antonenas V, Gottlieb DJ. 2006. Unrelated umbilical cord blood transplantation for adults with haematological malignancies: Results from a single Australian centre. Intern Med J 36:355–361.

Braiman L, Alt A, Kuroki T, Ohba M, Bak A, Tennenbaum T, Sampson SR. 2001. Activation of protein kinase C zeta induces serine phosphorylation of VAMP2 in the GLUT4 compartment and increases glucose transport in skeletal muscle. Mol Cell Biol 21:7852–7861.

Chen X, Al-Hasani H, Olausson T, Wenthzel AM, Smith U, Cushman SW. 2003. Activity, phosphorylation state and subcellular distribution of GLUT4-targeted Akt2 in rat adipose cells. J Cell Sci 116:3511–3518.

Chuang LY, Guh JY, Liu SF, Hung MY, Liao TN, Chiang TA, Huang JS, Huang YL, Lin CF, Yang YL. 2003. Regulation of type II transforming-growth-factor-beta receptors by protein kinase C iota. Biochem J 375:385–393.

Chung J, Grammer TC, Lemon KP, Kazlauskas A, Blenis J. 1994. PDGF- and insulin-dependent p70 S6K activation mediated by phosphatidylinositol-3-OH kinase. Nature 370:71–75.

Debili N, Robin C, Schiavon V, Letestu R, Pflumio F, Mitjavila-Garcia MT, Coulombel L, Vainchenker W. 2001. Different expression of CD41 on human lymphoid and myeloid progenitors from adults and neonates. Blood 97:2023–2030.

Fritsch G, Buchinger P, Printz D, Fink FM, Mann G, Peters C, Wagner T, Adler A, Gadner H. 1993. Rapid discrimination of early CD34+ myeloid progenitors using CD45-RA analysis. Blood 81:2301–2309.

Galetic I, Andjelkovic M, Meier R, Brodbeck D, Park J, Hemmings BA. 1999. Mechanism of protein kinase B activation by insulin/insulin-like growth factor-1 revealed by specific inhibitors of phosphoinositide 3-kinase—Significance for diabetes and cancer. Pharmacol Ther 82:409–425.

Goransson O, Wijkander J, Manganiello V, Degerman E. 1998. Insulin-induced translocation of protein kinase B to the plasma membrane in rat adipocytes. Biochem Biophys Res Commun 246:249–254.

Hao QL, Zhu J, Price MA, Payne KJ, Barsky LW, Crooks GM. 2001. Identification of a novel, human multilymphoid progenitor in cord blood. Blood 97:3683–3690.

Herr HJ, Bernard JR, Reeder DW, Rivas DA, Limon JJ, Yaspelkis BB3rd. 2005. Insulin-stimulated plasma membrane association and activation of Akt2, aPKC zeta and aPKC lambda in high fat fed rodent skeletal muscle. J Physiol 565:627–636.

Huang S, Chen Z, Yu JF, Young D, Bashey A, Ho AD, Law P. 1999. Correlation between IL-3 receptor expression and growth potential of human CD34+ hematopoietic cells from different tissues. Stem Cells 17:265–272.

Isotani S, Hara K, Tokunaga C, Inoue H, Avruch J, Yonezawa K. 1999. Immunopurified mammalian target of rapamycin phosphorylates and activates p70 S6 kinase alpha in vitro. J Biol Chem 274:34493–34498.

Kanayasu-Toyoda T, Yamaguchi T, Uchida E, Hayakawa T. 1999. Commitment of neutrophilic differentiation and proliferation of HL-60 cells coincides with expression of transferrin receptor. Effect of granulocyte colony stimulating factor on differentiation and proliferation. J Biol Chem 274:25471–25480.

Kanayasu-Toyoda T, Yamaguchi T, Oshizawa T, Kogi M, Uchida E, Hayakawa T. 2002. Role of the p70 S6 kinase cascade in neutrophilic differentiation and proliferation of HL-60 cells—a study of transferrin receptor-positive and -negative cells obtained from dimethyl sulfoxide- or retinoic acid-treated HL-60 cells. Arch Biochem Biophys 405:21–31.

Kanayasu-Toyoda T, Yamaguchi T, Oshizawa T, Uchida E, Hayakawa T. 2003. The role of c-Myc on granulocyte colony-stimulating factor-dependent neutrophilic proliferation and differentiation of HL-60 cells. Biochem Pharmacol 66:133–140.

Kanzaki M, Mora S, Hwang JB, Saltiel AR, Pessin JE. 2004. Atypical protein kinase C (PKCzeta/lambda) is a convergent downstream target of the insulin-stimulated phosphatidylinositol 3-kinase and TC10 signaling pathways. J Cell Biol 164:279–290.

Lafuente MJ, Martin P, Garcia-Cao I, Diaz-Meco MT, Serrano M, Moscat J. 2003. Regulation of mature T lymphocyte proliferation and differentiation by Par-4. Embo J 22:4689–4698.

Lallena MJ, Diaz-Meco MT, Bren G, Paya CV, Moscat J. 1999. Activation of IkappaB kinase beta by protein kinase C isoforms. Mol Cell Biol 19:2180–2188.

Liu WS, Heckman CA. 1998. The sevenfold way of PKC regulation. Cell Signal 10:529–542.

Manz MG, Miyamoto T, Akashi K, Weissman IL. 2002. Prospective isolation of human clonogenic common myeloid progenitors. Proc Natl Acad Sci USA 99:11872–11877.

Martin P, Duran A, Minguet S, Gaspar ML, Diaz-Meco MT, Rennert P, Leitges M, Moscat J. 2002. Role of zeta PKC in B-cell signaling and function. Embo J 21:4049–4057.

Mino E, Kobayashi R, Yoshida M, Suzuki Y, Yamada M, Kobayashi K. 2004. Umbilical cord blood stem cell transplantation from unrelated HLA-matched donor in an infant with severe congenital neutropenia. Bone Marrow Transplant 33:969–971.

Muscella A, Greco S, Elia MG, Storelli C, Marsigliante S. 2003. PKC-zeta is required for angiotensin II-induced activation of ERK and synthesis of C-FOS in MCF-7 cells. J Cell Physiol 197:61–68.

Nakanishi H, Brewer KA, Exton JH. 1993. Activation of the zeta isozyme of protein kinase C by phosphatidylinositol 3,4,5-trisphosphate. J Biol Chem 268:13–16.

Nakazawa Y, Sakashita K, Kinoshita M, Saida K, Shigemura T, Yanagisawa R, Shikama N, Kamijo T, Koike K. 2004. Successful unrelated cord blood transplantation using a reduced-intensity conditioning regimen in a 6-month-old infant with congenital neutropenia complicated by severe pneumonia. Int J Hematol 80:287–290.

Nguyen BT, Dessauer CW. 2005. Relaxin stimulates protein kinase C zeta translocation: Requirement for cyclic adenosine 3',5'-monophosphate production. Mol Endocrinol 19:1012–1023.

Ooi J. 2006. The efficacy of unrelated cord blood transplantation for adult myelodysplastic syndrome. Leuk Lymphoma 47:599–602.

Rappold I, Ziegler BL, Kohler I, Marchetto S, Rosnet O, Birnbaum D, Simmons PJ, Zannettino AC, Hill B, Neu S, Knapp W, Alitalo R, Alitalo K, Ullrich A, Kanz L, Buhring HJ. 1997. Functional and phenotypic characterization of cord blood and bone marrow subsets expressing FLT3 (CD135) receptor tyrosine kinase. Blood 90:111–125.

Romanelli A, Martin KA, Toker A, Blenis J. 1999. p70 S6 kinase is regulated by protein kinase Czeta and participates in a phosphoinositide 3-kinase-regulated signalling complex. Mol Cell Biol 19:2921–2928.

Sasaoka T, Wada T, Fukui K, Murakami S, Ishihara H, Suzuki R, Tobe K, Kadowaki T, Kobayashi M. 2004. SH2-containing inositol phosphatase 2 predominantly regulates Akt2, and not Akt1, phosphorylation at the plasma membrane in response to insulin in 3T3-L1 adipocytes. J Biol Chem 279:14835–14843.

Selbie LA, Schmitz-Peiffer C, Sheng Y, Biden TJ. 1993. Molecular cloning and characterization of PKC iota, an atypical isoform of protein kinase C derived from insulin-secreting cells. J Biol Chem 268:24296–24302.

Soloff RS, Katayama C, Lin MY, Feramisco JR, Hedrick SM. 2004. Targeted deletion of protein kinase C lambda reveals a distribution of functions between the two atypical protein kinase C isoforms. J Immunol 173:3250–3260.

Standaert ML, Bandyopadhyay G, Perez L, Price D, Galloway L, Poklepovic A, Sajan MP, Cenni V, Sirri A, Moscat J, Toker A, Farese RV. 1999. Insulin activates protein kinases C-zeta and C-lambda by an autophosphorylation-dependent mechanism and stimulates their translocation to GLUT4 vesicles and other membrane fractions in rat adipocytes. J Biol Chem 274:25308–25316.

Tenen DG, Hromas R, Licht JD, Zhang DE. 1997. Transcription factors, normal myeloid development, and leukemia. Blood 90:489–519.

Tisdale EJ. 2002. Glyceraldehyde-3-phosphate dehydrogenase is phosphorylated by protein kinase Ciota/lambda and plays a role in microtubule dynamics in the early secretory pathway. J Biol Chem 277:3334–3341.

Ward AC, Loeb DM, Soede-Bobok AA, Touw IP, Friedman AD. 2000. Regulation of granulopoiesis by transcription factors and cytokine signals. Leukemia 14:973–990.

Weng QP, Kozlowski M, Belham C, Zhang A, Comb MJ, Avruch J. 1998. Regulation of the p70 S6 kinase by phosphorylation in vivo. Analysis using site-specific anti-phosphopeptide antibodies. J Biol Chem 273:16621–16629.

Wooten MW, Vandenplas ML, Seibenhener ML, Geetha T, Diaz-Meco MT. 2001. Nerve growth factor stimulates multisite tyrosine phosphorylation and activation of the atypical protein kinase C's via a src kinase pathway. Mol Cell Biol 21:8414–8427.

Yamada K, Mizusawa M, Harima A, Kajiwara K, Hamaki T, Hoshi K, Kozai Y, Kodo H. 2006. Induction of remission of relapsed acute myeloid leukemia after unrelated donor cord blood transplantation by concomitant low-dose cytarabine and calcitriol in adults. Eur J Haematol 77:345–348.

Yamaguchi T, Mukasa T, Uchida E, Kanayasu-Toyoda T, Hayakawa T. 1999. The role of STAT3 in granulocyte colony-stimulating factor-induced enhancement of neutrophilic differentiation of Me2SO-treated HL-60 cells. GM-CSF inhibits the nuclear translocation of tyrosine-phosphorylated STAT3. J Biol Chem 274:15575–15581.

Genes and Environment, Vol. 28, No. 2 pp. 68–73 (2006)

Regular article

Microcystin-LR is not Mutagenic *in vivo* in the λ/*lacZ* Transgenic Mouse (Muta™Mouse)

Li Zhan[1,2], Masamitsu Honma[2], Li Wang[1], Makoto Hayashi[2], De-Sheng Wu[4], Li-Shi Zhang[4], Palanichamy Rajaguru[3,5] and Takayoshi Suzuki[2,3,6]

[1]National Chengdu Center for Safety Evaluation of Traditional Chinese Medicine, West China Hospital, Sichuan University, Chengdu, China
[2]Division of Genetics and Mutagenesis, [3]Division of Cellular and Gene Therapy Products, National Institute of Health Sciences, Tokyo, Japan
[4]West China School of Public Health, Sichuan University, Chengdu, China
[5]Department of Biotechnology, School of Engineering and Technology, Bharathidasan University, Tiruchirappalli, India

(Received April 2, 2006; Accepted April 18, 2006)

The water pollution of toxic cyanobacteria (blue-green algae) is causing a serious public health problem in many parts of the world. Microcystin-LR (MCLR) is a potent cyclic heptapeptidic hepatotoxin produced by the cyanobacterium *Microcystis aeruginosa*. MCLR presents acute and chronic hazards to human health and has been linked to primary liver cancer in humans chronically exposed to this peptide toxin through drinking water. To assess the *in vivo* mutagenecity of MCLR, the λ/*lacZ* transgenic mice (Muta™Mouse) were treated with MCLR (1 mg/kg per week x 4) and examined for mutant frequencies (MFs) in the *lacZ* and *cII* genes of liver and lungs. Micronucleus induction in peripheral blood cells was also assessed. Co-mutagenic effect of MCLR was studied in combination with *N*-nitrosodiethylamine (DEN). MCLR did not increase either MFs of the target genes in liver and lungs or micronucleus frequency in the peripheral blood cells of the λ/*lacZ* transgenic mouse. While DEN treatment increased MFs significantly, the co-administration of MCLR did not potentiate its mutagenicity. We conclude that pure MCLR has no *in vivo* mutagenicity as it failed to induce gene mutation and micronucleus in transgenic mouse. Its tumor promoting effect is independent of its interaction to DNA.

Key words: Microcystin-LR, *N*-nitrosodiethylamine, *lacZ*, *cII*, Muta™Mouse

Introduction

The water pollution of toxic cyanobacterial bloom (blue-green algae) is an increasing problem worldwide and worsens with eutrophication of drinking- and recreational- water reservoirs due to industrialization (1,2). Cyanobacteria produce lethal toxins, and often associated to death of livestock and cases of human illness caused by drinking water contaminated by these toxins, which have drawn the attention of the World Health Organization (WHO) (3). Microcystins are the most common group of cyanobacterial toxins comprised of over 60 structurally related cyclic heptapeptides (4) with potent hepatotoxicity and tumor promotion ability (5,6). Among them, Microcystin-LR (MCLR) is the most frequent secondary metabolite produced by *Microcystis aeruginosa* (2,7). MCLR presents acute and chronic hazards to human health (8,9). Although human illnesses attributed to microcystins include gastroenteritis and allergic/irritation reactions, the primary target of the toxin is the liver (10–14). It has been suspected to be involved with promotion of primary liver cancer in humans chronically exposed to doses of these peptide toxins through drinking water (15,16).

Algal toxins were reported to cause chromosomal breakages in human lymphocytes *in vitro* (17). Genotoxicity of cynobacterial extract has been demonstrated by SOS chromotest with *Escherichia coli* PQ37 and the comet assay with human lymphocytes (18) and in four strains of *Salmonella typhimurium* (TA97, TA98, TA100 and TA102) in Ames test with or without S9 mix (19). In the same study, however, pure MCLR did not show any mutagenicity in all these strains. MCLR was reported to damage the mitotic spindle apparatus and thus induces polyploidy and apoptosis and necrosis in Chinese hamster ovary (CHO-K1) cells (20), and to induce gene mutation with base substitution in human RSa cells (21). Recently we have demonstrated mutagenic and clastogenic activities of MCLR in human lymphoblastoid cells (TK6) after 24 h treatment *in vitro*

[6]Correspondence to: Takayoshi Suzuki, Division of Cellular and Gene Therapy Products, National Institute of Health Sciences, 1-18-1 Kamiyoga, Setagaya-ku, Tokyo 158-8501, Japan. Tel: +81-3-3700-1926, Fax: +81-3-3700-1926, E-mail suzuki@nihs.go.jp

(22). Because MCLR induced mainly LOH type mutations rather than point mutations, mutagenicity of MCLR might be exerted by a clastogenic mechanism. Nevertheless, *in vivo* genotoxicity of this cyanotoxin is less convincing and relatively undescribed. Therefore, the present study was conducted to evaluate the *in vivo* mutagenicity of MCLR using transgenic (TG) mouse mutation assay. TG system has been shown to be useful for studying chemical mutagenesis and clastogenesis *in vivo* (23–25). This is largely attributed to its ability to detect tissue-specific gene mutations. TG assay also permits analysis of mutation at the molecular level and allows examination of the relation between mutagenesis and carcinogeneis *in vivo* in detail (25). Since MCLR has been found to promote tumor initiated with *N*-nitrosodiethylamine (DEN) in rats (5), the co-mutagenic (potentiation) effects of MCLR in combination with DEN was also studied.

Materials and Methods

Chemicals: MCLR and DEN were purchased from Wako Pure Chemical Industries, Ltd. (Osaka, Japan). MCLR was dissolved in saline immediately before use. Phenyl-β-D-galactoside (P-gal) was purchased from Sigma.

Treatment of Muta™Mice: Male Muta™Mice (5-6-week old, ca. 25 g body weight) supplied by Covance Research Products (PA, USA) were acclimatized for 1 week before use. The animals were divided into 4 groups of 5 mice each and administered with weekly doses of either vehicle (saline), MCLR (1 mg/kg, 1/10 of LD_{50} in mice), DEN (25 mg/kg, 1/4 of LD_{50} in mice) or DEN + MCLR (25 mg/kg and 1 mg/kg, respectively) for 4 weeks. Saline and MCLR were administered intragastrically while DEN was intraperitonealy injected. No apparent sign of toxicity was observed in any mice.

Micronucleus assay in peripheral blood cells: Forty eight hours after the first treatment, 5 μL of peripheral blood was collected from the tail vein without anti-coagulant. The blood thus collected from each animal was placed on an acridine orange-coated glass slide, covered with a cover slip, and supravitally stained (26). Type I, II, and III reticulocytes (RETs) with red fluorescent reticulum in the cytoplasm were scored under a fluorescent microscope. One thousand RETs were examined per animal within a few days after the slide preparation. The number of RETs with micronucleus (MNRETs) was recorded.

Mutation assay: 1) Tissue collection: Mice were killed by cervical dislocation 7 days after the last treatment. Liver and lungs were removed, immediately frozen in liquid nitrogen, and stored at −80°C until DNA extraction. MFs of *lacZ/cII* transgenes derived from liver and lungs were determined as described previously (27–29). DNA sequencing of mutants isolated from the control and MCLR treated animals were carried out as described below.

2) Sequence analysis of *cII* gene: The *cII* mutant plaques were transferred into a microtube containing 50 μL SM buffer and 5 μL chloroform. The λ phage *cII* region was amplified directly from mutant plaque solution by Taq DNA polymerase (Takara Shuzo, Tokyo, Japan) with primers P1, 5′-AAAAAGGGCAT-CAAATTAAACC-3′; and P2, 5′-CCGAAGTTGAG-TATTTTTG- CTGT-3′. Amplification was done by the Minicycler PTC-150-25 (MJ Research, Inc., MA, USA) under the following thermal cycling: 95°C 5 min→ (95°C 20 s, 53°C 30 s, 72°C 40 s)×30 cycles→72°C 10 min. Amplification of 446 bp PCR product was checked by 2100 Bioanalyzer using lab DNA chips (Agilent Technologies, USA) and purified with a microspin column (Amersham Pharmacia, Tokyo, Japan) before being used for a sequencing reaction with the Ampli Taq cycle sequencing kit (PE Biosystems, Tokyo, Japan). The sequencing reaction was performed by Minicycler PTC-150-25 with 25 cycles of denaturing at 96°C for 10 s, annealing at 50°C for 5 s, and extension at 60°C for 4 min, with the primer P1. The reaction product was purified by ethanol precipitation and analyzed by the ABI PRISM® 310 Genetics Analyzer (PE Biosystems, Tokyo, Japan).

3) Statistical analysis: The results of the different treatment groups were compared using Students' *t*-test. Significance was indicated by P values <0.05.

Results

Micronucleus induction in peripheral blood: Results of the micronucleus test 48 h after the first administration of chemicals in the Muta™Mice is shown in Fig. 1. The mean frequency of MNRETs did not increase significantly ($P>0.05$) in any of the treatment group in comparison with that of the control group.

Mutant frequency of *lacZ* and *cII* genes: The mutant frequencies (MFs) observed in the DNA preparations extracted from the liver and lung tissues 7 days after the last treatment are shown in Table 1. In MCLR-treated mice, the MFs of *lacZ* and *cII* genes in liver were not different significantly ($P>0.05$) from that of the background levels. Although a slight increase was observed in the lungs, it was not statistically significant ($P>0.05$). DEN treatment significantly ($P<0.05$) increased MFs of both the target genes in both liver and lungs (for *lacZ* gene 6.1 fold and 3.7 fold respectively and for *cII* gene 11.0 fold and 4.6 fold, respectively). We did not observe significant difference in MFs between DEN-treated and DEN+MCLR co-treated animals.

***cII* mutation spectrum:** Thirty four MCLR-in-

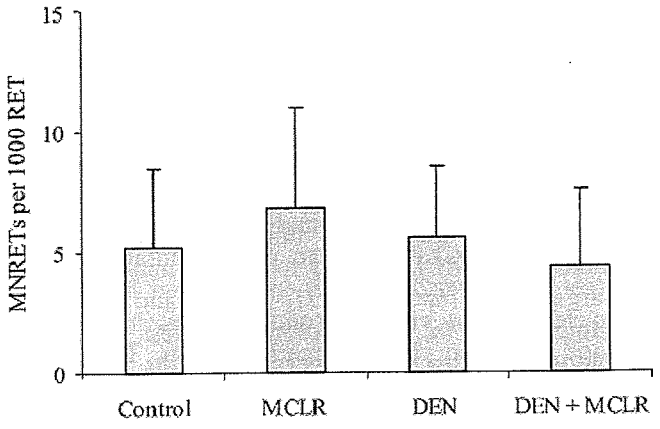

Fig. 1. Incidence of MNRET in the peripheral blood of Muta™Mouse 48 h following treatment with MCLR (1 mg/kg), DEN (25 mg/kg) and DEN (25 mg/kg) + MCLR (1 mg/kg).

duced and 46 DEN-induced mutants together with 42 spontaneous mutants from the liver were subjected to sequence analysis. The mutation spectra are summarized in Table 2. Spontaneous mutations consisted mainly of base substitutions (37/42). Among them, G:C to A:T transitions (21/26) predominated and most of them (17/21) occurred at CpG sites. DEN-induced mutations also consisted mainly of base substitutions (42/46). Compared to the control, G:C to A:T transitions were decreased in DEN treated group (50% versus 24% respectively) while A:T to T:A transversions were increased (2% versus 28%, respectively). However no obvious change was observed for incidences of mutations induced by MCLR including transitions (62% versus 62%) and transversions (27% versus 21%).

Table 1. MFs in the *lacZ* and *cII* gene from liver and lung of Muta™Mouse treated with MCLR (1 mg/kg), DEN (25 mg/kg) and DEN (25 mg/kg) + MCLR (1 mg/kg)

Organ	Treatment	*lacZ*				*cII*			
		Total plaques	Mutants	MF ($\times 10^{-6}$)	Mean ± SD	Total plaques	Mutants	MF ($\times 10^{-6}$)	Mean ± SD
Liver	Control	3311250	138	41.7	43.8 ± 11.7	3486000	69	19.8	20.5 ± 8.2
	MCLR	4053750	173	42.7	40.3 ± 13.7	4282500	94	21.9	21.1 ± 3.5
	DEN	3175000	963	261.7	268.4 ± 62.4*	3,495,000	788	225.5	226.6 ± 54.2*
	DEN + MCLR	2122500	472	222.4	206.9 ± 83.4†	2,149,500	391	181.9	176.4 ± 77†
Lung	Control	3823750	144	28.8	32.1 ± 13.9	4305000	110	25.6	25.7 ± 4.3
	MCLR	3823750	134	35.0	35.7 ± 4.89	2468250	93	37.7	36.9 ± 21.3
	DEN	3622500	416	114.8	117.5 ± 17.2*	2874000	332	115.5	118.1 ± 10.1*
	DEN + MCLR	2576250	264	102.5	109.9 ± 44.7†	1,136,250	141	124.1	132.2 ± 20.6†

*Compared to the control group $P < 0.05$
†Compared to the DEN-treated group $P > 0.05$

Table 2. Summary of *cII* mutations in the liver of control, MCLR- and DEN-treated Muta™Mice

Mutation class	Liver					
	Control	CpG	MCLR (%)	CpG	DEN (%)	CpG
Base	37 (89)		28 (82)		42 (91)	
Transitions	*26 (62)*		*21 (62)*		*20 (43)*	
G:C to A:T	21 (50)	17 (40)	20 (59)	17 (52)	11 (24)	6 (13)
A:T to G:C	5 (12)		1 (3)		9 (20)	
Transversions	*11 (27)*		*7 (21)*		*22 (48)*	
A:T to T:A	1 (2)		1 (3)		13 (28)	
A:T to C:G	4 (10)		2 (6)		2 (4)	
G:C to T:A	4 (10)		4 (12)		7 (15)	
G:C to C:G	2 (5)		0 (0)		0 (0)	
−1 Frameshift	1 (2)		2 (6)		1 (2)	
+1 Frameshift	3 (7)		4 (12)		0 (0)	
Deletion	0 (0)		0 (0)		1 (2)	
Insertion	0 (0)		0 (0)		0 (0)	
Complex	1 (2)		0 (0)		2 (4)	
Total	42 (100)		34 (100)		46 (100)	
MF ($\times 10^{-6}$)	43.8		40.3		268.4	

Discussion

The occurrence of toxic cyanobacterial blooms found in eutrophic, municipal, and residential water supplies is an increasing public health problem. Frequent deaths of domestic and wild animals are caused by drinking water contaminated by lethal toxins produced by cynobacteria. MCLR is the most commonly encountered and among the most toxic algal cyclic peptide hepatotoxins. Epidemiological studies have indicated a close relationship between primary liver cancer in human and cynobacteria contaminated drinking water (15,16). While there are several reports showing the *in vitro* genotoxicity of MCLR (21,22) or cyanobacterial extract (18,19), the evidence for the *in vivo* genotoxicity of this toxin is less convincing. Therefore, the main objectives of this study were to assess the *in vivo* genotoxicity of MCLR (if any) and its role in potentiation of DEN induced mutations for its suggested tumor promoting effects. To meet out these objectives male Muta^{TM}Mouse were administered with MCLR alone or in combination with DEN and examined for two end points- point mutation in transgenes, and micronucleus induction in peripheral blood cells. Considering the strong correlation between organ specific genotoxicty and organ specific carcinogenicity, the assessment of genotoxicity in multiple organs *in vivo* may indicate its target organ in humans and provide useful information for the evaluation of chemical safety. In the present research, hence, two target organs -liver and lungs- were examined for the evidence for mutagenicity.

Intraperitoneal injection of the raw cyanobacterial extracts containing several other microcystins besides MCLR induced micronucleus in the mouse bone marrow cells (19) and degradation and fragmentation of DNA in the liver cells (30). In the present study a pure MCLR (1 mg/kg = 1/10 of LD_{50}) was used, but no mutagenicity was observed. In another study, neoplastic nodule formation has been observed in the livers of mice received 100 intraperitoneal injections of sublethal doses of MCLR (20 μg/kg) over a period of 28 weeks (31). In the same study, oral administration of relatively higher doses of MCLR (80 μg/kg) under similar experimental conditions did not induce characteristic chronic injuries. Similarly, as suggested by the authors, fragmentation of DNA observed in hepatocytes of mice treated with the extract or MCLR (0.5–2.0 folds of LD_{50} doses) might be a consequence of endonucleolytic DNA degradation associated with cytotoxicity, rather than by a direct toxin-DNA interaction (30). In support to this, recently Zegura *et al.* (32) have reported that the genotoxicity of MCLR could be mediated by reactive oxygen species. So it may be inferred that some other mutagenic toxins present in the extracts or different routes of administration might be responsible for the positive results observed in those studies. However, MCLR treatment caused enhanced formation of 8-oxo-7,8-dihydro-2′-deoxyguanosine in a time- and dose-dependent manner *in vitro* in primary cultured hepatocytes and *in vivo* in rat liver cells that could involve in the formation of hepatic tumors during long-term exposure to this cyanobacterial hepatotoxin (33). In contrast, in our study, under present experimental conditions, MCLR failed to induce mutation in both target genes (*lacZ* and *cII*) in liver and lungs of TG mouse. The *in vivo* micronucleus test in peripheral blood cells also yielded negative results. These results indicate that MLCR is capable of inducing neither point mutation nor chromosomal breakage *in vivo* in mouse organs.

It is widely believed that MCLR has tumor promoting effect (5,6). To test the possible potentiating effect of MCLR on mutagenicity of DEN, in our study, mice were simultaneously treated with DEN (25 mg/kg) and MCLR (1 mg/kg) once a week for four weeks. Relative to control mice, no significant increase in micronucleus frequency was observed either in DEN- or DEN+ MCLR-treated mice. This is in consistent with the negative results observed with DEN as previously reported (24). Further, simultaneous administration of MCLR with DEN did not increase MF caused by DEN in either of the target genes, although DEN treatment resulted in a significant increase in MFs in both *lacZ* and *cII* genes from liver and lungs. This indicates that the tumor promoting effects of MCLR is independent of mutagenicity of DEN. Because MCLR is known as an inhibitor of protein phosphatase 1 and 2A (5,34), the tumor promoting activity might be exerted by a disturbance of protein phosphorylation. Okadaic acid, which is known as a tumor promoter and a strong inhibitor of protein phosphatases (35), has similar mutagenic properties as MCLR (non-mutagenic in Salmonella and mutagenic in mammalian cells (36,37)). It is possible that tumor promoting activity of both compounds has a common mechanism through the inhibition of protein phosphatases.

In conclusion, pure MCLR has no *in vivo* genotoxicity as it is failed to induce gene mutation and micronucleus in transgenic mouse. Also lack of potentiation of DEN induced mutations in transgenes, as observed in the present study, indicates that the tumor promoting effects of MCLR is independent of its interaction to DNA.

Acknowledgement: This work was supported by a grant from the Japan-China Sasagawa Medical Fellowship and a Grant-in-Aid for Scientific Research from the Ministry of Health, Labour and Welfare of Japan.

References

1 Carmichael WW. Toxins of freshwater algae. In: Tu AT,

editor. Handbook of natural toxins. New York: Marcel Dekker; 1988. p. 121–47.
2 Codd GA, Bell SG, Kaya K, Ward CJ, Beattie KA, Metcalf JS. Cyanobacterial toxins, exposure routs and human health. Eur J Phycol. 1999; 34: 405–15.
3 Chorus I. Introduction: cyanotoxins-research for environment safety and human health. In: Chorus I, editor. Cyanotoxins. Germany: Springer; 2001. p. 1–4.
4 Carmichael WW. Health effects of toxin-producing cyanobacteria: the CyanoHABs. Hum. Ecol Risk Assess. 2001; 7: 1393–407.
5 Nishiwaki-Matsushima R, Ohta T, Nishiwaki S, Suganuma M, Kohyama K, Ishikawa T, Carmichael WW, Fujiki H. Liver tumor promotion by the cyanobacteria cyclic peptide toxin microcystin-LR. J Cancer Res Clin Oncol. 1992; 118: 420–4.
6 Carmichael WW. The toxins of cyanobacteria. Sci Am. 1994; 270: 78–86.
7 Carmichael WW. Cyanobacteria secondary metabolites: the cyanotoxins. J Appl Bacteriol. 1992; 72: 445–59.
8 Carmichael WW. The cyanotoxins. In: Callow JA editor. Advances in botanical research. London: Academic Press; 1997. p. 211–56.
9 Hernandez M, Macia M, Padilla C, Del Campo F. Modulation of human polymorphonuclear leukocyte adherence by cyanopeptide toxin. Environ Res Sci. 2000; 84: 64–8.
10 Codd GA, Ward CJ, Bell SG. Cyanobacterial toxins: occurrence, modes of action, health effects and exposure routes. Arch Toxicol Suppl. 1997; 19: 399–410.
11 Miura GA, Robinson NA, Geisbert TW, Bostian KA, White JD, Pace JG. Comparison of *in vivo* and *in vitro* toxic effects of microcystin-LR in fasted rats. Toxicon. 1989; 27: 1229–40.
12 Rao PVL, Bhattacharya R, Parida MM, Jana AM, Bhaskar AS. Freshwater cyanobacterium *Microcystis aeruginosa* (UTEX 2385) induced DNA damage *in vivo* and *in vitro*. Environ Toxicol Pharmacol. 1998; 5: 1–6.
13 Bhattacharya R, Rao PV, Bhaskar AS, Pant SC, Dube SN. Liver slice culture for assessing hepatotoxicity of freshwater cyanobacteria. Hum Exp Toxicol. 1996; 15: 105–10.
14 Ding WX, Shen HM, Zhu HG, Ong CN. Studies on oxidative damage induced by cyanobacteria extract in primary cultured rat hepatocytes. Environ Res. 1998; 78: 12–8.
15 Yu SZ. Primary prevention of hepatocellular carcinoma. J Gastroenterol Hepatol. 1995; 10: 674–82.
16 Ueno Y, Nagata S, Tsutsumi T, Hasegawa A, Watanabe MF, Park HD, Chen GC, Chen G, Yu SZ. Detection of microcystins, a blue-green algal hepatotoxin, in drinking water sampled in Haimen and Fusui, endemic areas of primary liver cancer in China, by highly sensitive immunoassay. Carcinogenesis 1996; 17: 1317–21.
17 Repavich WM, Sonzongni WC, Standridge JH, Wedephohl RE, Meisner LF. Cyanobacteria (blue-green algae) in Wisconsin waters: acute and chronic toxicity. Water Res. 1990; 24: 225–31.
18 Mankiewicz J, Walter Z, Tarczynska M, Palyvoda O, Wojtysiak-Staniaszczyk M, Zalewski M. Genotoxicity of cyanobacterial extracts containing microcystins from Polish water reservoirs as determined by SOS chromotest and comet assay. Environ Toxicol. 2002; 17: 341–50.
19 Ding WX, Shen HM, Zhu HG, Lee BL, Ong CN. Genotoxicity of microcystic cyanobacteria extract of a water source in China. Mutat Res. 1999; 442: 69–77.
20 Lankoff A, Banasik A, Obe G, Deperas M, Kuzminski K, Tarczynska M, Jurczak T, Wojcik A. Effect of microcystin-LR and cyanobacterial extract from Polish reservoir of drinking water on cell cycle progression, mitotic spindle, and apoptosis in CHO-K1 cells. Toxicol Appl Pharmacol. 2003; 189: 204–13.
21 Suzuki H, Watanabe MF, Wu Y, Sugita T, Kita K, Sato T, Wang X, Tanzawa H, Sekiya S, Suzuki N. Mutagenicity of microcystin-LR in human RSa cells. Int J Mol Med. 1998; 2: 109–12.
22 Zhan L, Sakamoto H, Sakuraba M, Wu de S, Zhang LS, Suzuki T, Hayashi M, Honma M. Genotoxicity of microcystin-LR in human lymphoblastoid TK6 cells. Mutat Res. 2004; 557: 1–6.
23 Douglas GR, Gingerich JD, Gossen JA, Bartlett SA. Sequence spectra of spontaneous *lacZ* gene mutations in transgenic mouse somatic and germline tissues, Mutagenesis 1994; 9: 451–8.
24 Suzuki T, Hayashi M, Sofuni T. Initial experiences and future directions for transgenic mouse mutation assays. Mutat Res. 1994; 307: 489–94.
25 Nohmi T, Suzuki T, Masumura K. Recent advances in the protocols of transgenic mouse mutation assays. Mutat Res. 2000; 455: 191–215.
26 Hayashi M, Morita T, Kodama Y, Sofuni T, Ishidate Jr. M. The micronucleus assay with mouse peripheral blood reticulocytes using acridine orange-coated slides. Mutat Res. 1990; 245: 245–9.
27 Suzuki T, Wang X, Miyata Y, Saeki K, Kohara A, Kawazoe Y, Hayashi M, Sofuni T. Hepatocarcinogen quinoline induces G:C to C:G transversions in the *cII* gene in the liver of lambda/lacZ transgenic mice (Muta™ Mouse). Mutat Res. 2000; 456: 73–81.
28 Kohara A, Suzuki T, Honma M, Ohwada T, Hayashi M. Mutagenicity of aristolochic acid in the *lambda/lacZ* transgenic mouse (Muta™Mouse). Mutat Res. 2002; 515: 63–72.
29 Yamada K, Suzuki T, Kohara A, Hayashi M, Hakura A, Mizutani T, Saeki K. Effect of 10-aza-substitution on benzo[*a*]pyrene mutagenicity *in vivo* and *in vitro*. Mutat Res. 2002; 521: 187–200.
30 Rao PV, Bhattacharya R. The cyanobacterial toxin microcystin-LR induced DNA damage in mouse liver *in vivo*. Toxicology 1996; 114: 29–36.
31 Ito E, Kondo F, Terao K, Harada I. Neoplastic nodular formation in mouse liver induced by repeated intraperitoneal injections of microcystin-LR. Toxicon. 1997; 35: 1453–7.
32 Zegura B, Lah TT, Filipic M. The role of reactive oxygen species in microcystin-LR-induced DNA damage. Toxicology 2004; 200: 59–68.
33 Bouaicha N, Maatouk I, Plessis MJ, Perin F. Genotoxic potential of Microcystin-LR and nodularin *in vitro* in primary cultured rat hepatocytes and *in vivo* in rat liver. Environ Toxicol. 2005; 20: 341–7.

34 Guzman RE, Solter PF, Runnegar MT. Inhibition of nuclear protein phosphatase activity in mouse hepatocytes by the cyanobacterial toxin microcystin-LR. Toxicon. 2003; 41: 773–81.
35 Gehringer MM. Microcystin-LR and okadaic acid-induced cellular effects: a dualistic response. FEBS Lett. 2004; 557: 1–8.
36 Aonuma S, Ushijima T, Nakayasu M, Shima H, Sugimura T, Nagao M. Mutation induction by okadaic acid, a protein phosphatase inhibitor, in CHL cells, but not in S. typhimurium. Mutat Res. 1991; 250: 375–81.
37 Nakagama H, Kaneko S, Shima H, Inamori H, Fukuda H, Kominami R, Sugimura T, Nagao M. Induction of minisatellite mutation in NIH 3T3 cells by treatment with the tumor promoter okadaic acid. Proc Natl Acad Sci U S A. 1997; 94: 10813–6.

TOXICOLOGICAL SCIENCES 94(1), 83–91 (2006)
doi:10.1093/toxsci/kfl075
Advance Access publication August 3, 2006

Flow Cytometric Analysis of Micronuclei in Peripheral Blood Reticulocytes: I. Intra- and Interlaboratory Comparison with Microscopic Scoring

Stephen D. Dertinger,* Michelle E. Bishop,† James P. McNamee,‡ Makoto Hayashi,§ Takayoshi Suzuki,§ Norihide Asano,¶ Madoka Nakajima,‖ Junichiro Saito,‖‖ Martha Moore,† Dorothea K. Torous,* and James T. MacGregor‖‖‖,[1]

Litron Laboratories, Rochester, New York 14623; †U.S. Food and Drug Administration, National Center for Toxicological Research, Jefferson, Arkansas 72079; ‡Health Canada, Ottawa, Ontario, Canada K1A 0L2; §National Institute of Health Sciences, Tokyo 158-8501, Japan; ¶Nitto Denko Corporation, Osaka 567-8680, Japan; ‖An-Pyo Center, Shizuoka 437-1213, Japan; ‖‖Astellas Pharma Inc., Tokyo 174-8511, Japan; ‖‖‖U.S. Food and Drug Administration, National Center for Toxicological Research, Rockville, Maryland 21012

Received February 2, 2006; accepted July 31, 2006

Accumulating evidence suggests that reticulocytes (RETs) in the peripheral blood of rats may represent a suitable cell population for use in the micronucleus assay, despite the ability of the rat spleen to selectively remove micronucleated erythrocytes from the peripheral circulation. To evaluate the analytical performance of a previously described flow cytometric method (Torous *et al.*, 2003, *Toxicol. Sci.* 74, 309–314) that may allow this assay to be conducted using peripheral blood *in lieu* of bone marrow sampling, we compared the sensitivity and performance characteristics of the flow cytometric technique with two established microscopy-based scoring methods. Peripheral blood samples from single Sprague-Dawley rats treated for 6 days with either vehicle or cyclophosphamide were prepared in replicate for scoring by the three methods at different laboratories. These blood-based measurements were compared to those derived from bone marrow specimens from the same animals, stained with acridine orange, and scored by microscopy. Through the analysis of replicate specimens, inter- and intralaboratory variability were evaluated for each method. Scoring reproducibility over time was also evaluated. These data support the premise that rat RETs harvested from peripheral blood are a suitable cell population to assess genotoxicant-induced micronucleus formation. The interlaboratory comparison provides evidence of the general robustness of the micronucleus endpoint using different analytical approaches. Furthermore, data presented herein demonstrate a clear advantage of flow cytometry–based scoring over microscopy—significantly lower inter- and intralaboratory variation and higher statistical sensitivity.

Key Words: flow cytometric analysis; reticulocytes; micronucleus test; CD71.

The *in vivo* rodent erythrocyte micronucleus (MN) test is widely used in research and regulatory safety assessment to evaluate the potential of chemical and physical agents to cause chromosomal damage. Historically, MN studies based on rat peripheral blood have been avoided as it has been assumed that the efficiency by which the rat spleen filters out erythrocytes with intracellular inclusions would reduce assay sensitivity (Hayashi *et al.*, 2000; Wakata *et al.*, 1998). However, accumulated data suggest that peripheral blood from intact rats can be used effectively to detect chemical-induced genotoxicity (Abramsson-Zetterberg *et al.*, 1999; Asanami *et al.*, 1995; Hamada *et al.*, 2001; Hayashi *et al.*, 1992; Hynes *et al.*, 2002; Romagna and Staniforth, 1989; Torous *et al.*, 2000, 2003; Wakata *et al.*, 1998). Thus, it appears that MN studies using peripheral blood sampling in the rat have the potential to substitute for labor-intensive, bone marrow–based tests. In addition, the ability to use low-volume blood samples will facilitate integration of the assay into routine toxicology and/or pharmacokinetic studies and may make it unnecessary to conduct separate assays for the evaluation of chromosomal damage (Asanami *et al.*, 1995; Hamada *et al.*, 2001; MacGregor *et al.*, 1995; Wakata *et al.*, 1998).

Before rat blood–based MN assays gain wider acceptance, especially in the context of regulatory testing requirements, additional information that allows direct comparisons between bone marrow and blood data is needed. Furthermore, the performance characteristics of the most widely utilized scoring techniques require further study. The experiments described herein were designed to address these issues of analytical performance by directly comparing values in blood and bone marrow obtained at different laboratories with three widely used methodologies, comparing values derived from two microscopy-based methods with a flow cytometry–based method that incorporates a calibration standard.

For each of the three scoring techniques, at least three proficient laboratories received replicate, coded samples for reticulocyte

[1] To whom correspondence should be sent at the present address: Toxicology Consulting Services, 201 Nomini Drive, Arnold, MD 21012. Fax: 410-975-0481. E-mail: jtmacgregor@earthlink.net.